ENHANCEMENT AND CHARACTERIZATION OF CANCEROUS TISSUE USING COMPUTED TOMOGRAPHY IMAGES

A Dissertation submitted in fulfillment of the requirements for the Degree
of

MASTER OF ENGINEERING
in
Electronic Instrumentation & Control Engineering

Submitted by

Kanika Sharma
801351008

Under the Guidance of
Dr. Deepti Mittal
Assistant Professor, EIED

2015

Electrical and Instrumentation Engineering Department
Thapar University, Patiala
(Declared as Deemed-to-be-University u/s 3 of the UGC Act., 1956)
Post Bag No. 32, Patiala – 147004
Punjab (India)

DECLARATION

I hereby certify that the work which is presented in dissertation entitled, **"Enhancement and Characterization of Cancerous Tissue Using Computed Tomography Images"**, in partial fulfillment of the requirements for the award of the degree of Master of Engineering in **Electronics Instrumentation and Control**, submitted to Electrical & Instrumentation Engineering Department of Thapar University, Patiala is as authentic record of my own work carried under the supervision of **Dr. Deepti Mittal**. It refers others researcher's work which are duly listed in the reference section. The matter contained in this dissertation has not been submitted, neither in part or in full to any other degree to any other university or institute except as reported in text and references.

Place: TU, Patiala
Date: 15 July 2015

Kanika Sharma
Roll No.: 801351008

It is certified that the above statement made by the student is correct to the best of my knowledge and belief.

Date: 15 July 2015

Dr. Deepti Mittal
Assistant Professor
Electrical & Instrumentation Engineering Department
Thapar University, Patiala

Countersigned by:

Head
Electrical & Instrumentation Engineering Department
Thapar University, Patiala

Dean (Academic Affairs)
Thapar University, Patiala

ACKNOWLEDGMENT

In pursuit of this academic endeavor, I feel that I have been singularly fortunate because inspiration, guidance, direction, cooperation, love and care - all came in my way in abundance and it seems almost an impossible task for me to acknowledge the same in adequate term.

I am very thankful to the Director of Thapar University, **Dr. Prakash Gopalan**, and our Head of the Department, **Dr. Ravinder Agarwal**, Department of Electrical and Instrumentation Engineering for their support during the research work.

Also, I shall be failing in my duty if I do not record my profound sense of indebtedness and heartfelt gratitude to my supervisor, **Dr. Deepti Mittal**, Assistant Professor, Department of Electrical and Instrumentation Engineering, Thapar University, Patiala, who guided and inspired me in pursuance of this work. It was her able supervision, advice, and guidance from the very early stage of this research as well as giving me extraordinary experiences throughout the work which has resulted in fruitful outcome. I feel bereft of words to acknowledge her contribution to shape my academic perceptivity.

I feel thankful to the entire faculty and staff of the Department of Electrical and Instrumentation Engineering. I would also like to thank my friends who devoted their valuable time and helped me in all possible ways towards successful completion of this work. I thank all those who have contributed directly or indirectly to this work.

Lastly, I would like to thank my parents for their unconditional support and encouragement.

KANIKA SHARMA

Roll No. 801351008

TABLE OF CONTENTS

LIST OF TABLES

LIST OF FIGURES

ABBREVIATION

CT – Computed Tomography

HCC – Hepatocellular Carcinoma

HE – Histogram Equalization

HECVO – Histogram Equalization with Constrained Variable Offset

MOBCS – Modified Object based Contrast Stretching

OAI – Object Approximation Image

OEI – Object Error Image

FOS – First Order Statistics

GLCM – Gray Level Co-occurrence Matrix

GLRLM – Gray Level Run Length Matrix

GTDM – Gray Tone Difference Matrix

SVM – Support Vector Machine

ABSTRACT

Computed tomography (CT) scan is most common imaging modality for diagnosis of various types of the diseases. The diagnosis of disease using CT images is done in two ways, one by visual inspection and other by computer aided diagnosis. The high quality of visible details is required in CT images for visual inspection by radiologists. For high quality CT images enhancement is required. The information present in the CT scan of tissues exists in the texture part of the CT images. CT images have good structural details but textural details need enhancement. The images obtained after enhancement assists radiologist to diagnose the disease easily and with less fatigue. The present work proposed two enhancement methods for CT images. First method is based on the transformation function of histogram equalization and it is modified by adding constrained variable offset to preserve the over enhancement produced by histogram equalization. This method improves the visual quality of the images and tumor is clearly visible in comparison to the original image. The second method is modified object based contrast stretching. In this method, first image is segmented using watershed method then it is divided into parts, object approximation image (OAI) and object error image (OEI). OEI is enhanced using greedy iterative stretching, and then mean adjustments are made to enhanced OEI and original OAI. To obtain final enhanced results both the images are added. The second method enhances the textural details of the CT images. Both methods are applied on 197 liver CT images database. The objective evaluation of both methods is done by quantitative performance measures. The evaluation shows that modified object based contrast stretching method (MOBCS) is better in comparison to histogram equalization with constrained variable offset (HECVO). To verify the textural enhancement of both method texture feature extraction is done using various feature extraction methods. Then feature selection is done using box plot study and sequential feature selection method. Feature selection show that HECVO method is not suitable for the texture feature analysis, so further work is done using results of MOBCS method. Classification of normal and abnormal liver tissue is done using support vector machine. The experimental results show that MOBCS performs better than original image in classifying the normal and abnormal tissue of the CT image.

CHAPTER 1

INTRODUCTION

The basic information related to computed tomography scans and objective of the present work is elucidated in the following sections of the chapter.

1.1 X-Ray COMPUTED TOMOGRAPHY

X-Ray computed tomography scan (CT scan) is very popular and common medical imaging modality. It is a non destructive method that uses computer processed X-Rays to visualize the inner parts of opaque objects. The three dimensional digital image is formed using digital geometry processing by taking large series of two dimension images of the object taken around single axis of rotation. It is used for diagnosis and therapeutic purposes in medical discipline. Mostly CT scan is used for diagnosis of various body parts such as head, lungs, cardiac, abdominal and pelvic, and extremities. In head mostly CT scan is used to detect infraction, calcification, bone trauma, tumor etc, in internals of lungs both acute and chronic changes can be detected, in heart coronary artery can be imaged, complex fractures can also be detected by the CT scan.

1.1.1. Basic principle and image formation

The basic principle of formation of an image by CT scan is it converts the physical contrast of the body to the image contrast. Physical contrast means the difference in density of the tissues present in the body. According to the density of the tissue, it will absorb or refract the radiation, by this difference in absorption and refraction image is formed. The soft tissue will be darker and the hard body parts will be brighter in the grayscale image formed by the machine. CT image formation process is shown in Figure 1.1.

The formation of image by CT scan is a three phase process:

- Scan Phase: the first phase is scanning the object or body and acquiring the data related to the body part and storing it in the computer’s memory. In the scan phase there are two distinct motions of the x-ray beam relative to the patient's body, one is the rotation of the x-ray tube and x-ray beam around the body and the other is scanning along the length of the patient and is achieved by moving the body through the scanner while the beam is rotating around it. It is the combination of these two motions that produce the complete set of data from which the images can be reconstructed.

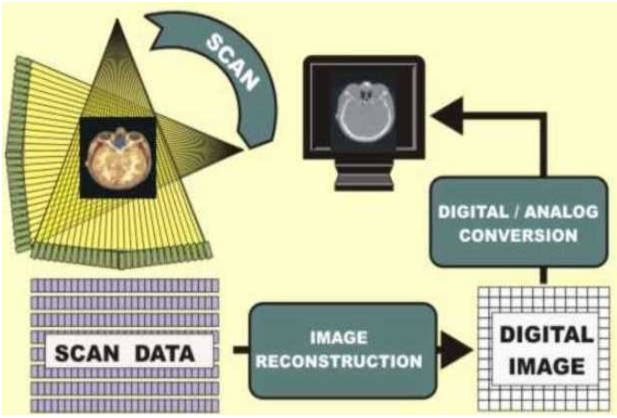

Figure 1.1 CT image formation [1]

- Image Reconstruction Phase: the second phase is image reconstruction. CT image reconstruction is a mathematical process for converting the scan data into a digital image of a specific anatomical area. Most images are created with the filtered back-projection method or sometimes with an enhanced process generally known as iterative reconstruction. During the reconstruction process each slice is formed and divided into a matrix of voxels (volume elements).
- Display Image Phase: the third phase is display phase in which the reconstructed data is converted to the digital form which can be displayed on the display screen. The image obtained from CT scan equipment is in Digital Imaging and Communications in Medicine (DICOM) format, which has very high dynamic range. This CT data set is reduced and converted to gray scale range (0-255 pixels) for display or printing purposes.

1.1.2. Image Quality and Its Characteristics

The quality of image obtained by CT scan plays an important role in the diagnostic purposes [1]. There are basic five image quality characteristics of the CT image:

- Contrast Sensitivity: It determines the range of visibility with respect to physical contrast. It controls the conversion of the physical contrast within the body to the visible contrast in an image.

- Visibility of Detail: It allows to visualize the details present in the image and blurring of image effects the visibility. In the CT imaging process there are several sources of blurring that collectively limit visibility of detail.

- Visual Noise: All medical imaging methods produce images with some visual noise. This is generally an undesirable characteristic that reduces visibility of certain types of objects and structures.

- Artifacts: An artifact is generally something that appears in an image that is not a direct visualization of an object or structure in the body.

- Spatial or geometric characteristics of the image: Slice thickness of the reconstructed image is included in the spatial characteristics. The quality of image also depends on this characteristic.

Characteristics of image quality are shown in Figure 1.2.

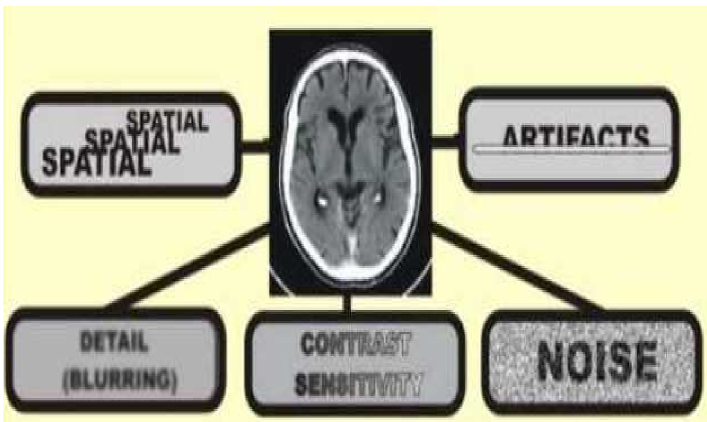

Figure 1.2 CT quality characteristics [1]

1.2 ENHANCEMENT OF CT IMAGES

The basic understanding of enhancement and the need of enhancement for CT images is explained in this section.

1.2.1 Image enhancement

Image enhancement is the technique to improve the quality of the image without any knowledge of source of degradation. The quality of image depends on the various factors such as contrast, noise, artifacts, spatial resolution and blurring. By adjusting one of the characteristics of the image quality, the quality of image can be improved. One of the most important characteristics of the image quality is contrast. Contrast enhancement improves the visibility of details in the image. The purpose of image enhancement is to make the image useful for both human observer and machine recognition. Basically image enhancement methods are divided into two categories:

- Spatial domain method: in this type of method, directly pixels of the image are modified according to the enhancement criteria to fulfill the purpose of enhancement.
- Frequency domain method: in this type of method, modification in image is made by first converting the image data in frequency domain and then applying the transformation function. To obtain the final enhanced image, data is again converted to spatial domain from frequency domain.

1.2.2 Need of enhancement for CT images

The diagnosis of disease through CT images is done by visual inspection by doctor. So the details present in the CT image must be superior for high quality inspection. Enhancement of CT images is required to improve the visibility of details present in the image, so that diagnosis of disease becomes easier. Enhancement of CT images also improves the textural details and the main information of the disease is present in the textural portion of the CT images. In CT scan a large set of data is obtained for one person for diagnosis. Doctor needs to study all the images to find the disease of the patient. If there is a small tumor or object causes disease, then a careful visual inspection is required by the doctor, to detect the disease in its prior stage, this takes a lot of time. In a day, doctor has many patients with the severe diseases, so if the CT images have high quality information and textural details with very effective contrast which visualizes the fine details of the body part, then doctor need not spend much time for one set of CT image data and the disease (tumor) can be detected in its primary stage.

The enhancement of CT images also assists in computer aided diagnosis for better detection of disease. Enhancement improves the efficiency of computer aided diagnosis and the radiologists can detect the disease in patient with greater accuracy in less time and at early stage easily.

In brief, enhancement of CT images is required for better and easy diagnosis of disease by doctor with less fatigue. Enhancement of CT images assists radiologists to detect even small tumors and also increases the efficiency of computer aided diagnosis.

CHAPTER 2

LITERATURE REVIEW

The literature review is divided into two categories, one includes the literature related to the enhancement of images and other is related to texture feature extraction and classification. The various image enhancement methodologies have been proposed in literature and some of them are shown as follows:

Y. Yu and H. Zhao [2] proposed a novel technique of enhancement of thoracic CT images to detect early stage lung cancer. First segmentation is performed using gray scale thresholding, then morphological operations and texture based segmentation are performed and then finally contrast limited adaptive histogram equalization enhancement method is applied. The algorithm is tested on 882 thoracic CT scan images. The enhancement filter designed is useful in automatic detection of lung nodules for CT images and also for other medical images.

A.H. Mir et al. [3] proposed a method to enhance the CT images based on texture features and fuggy logic. The texture features are extracted to obtain the disease related information and then fuzzy logic based enhancement operator is applied to enhance the details of disease to detect cancer in its early stage. The proposed method is tested on 100 CT scans of liver.

I. Jafar and H. Ying [4] proposed an enhancement methodology based on histogram equalization. Variational formulation of histogram equalization is obtained and then a constraint is added to the transformation function of variational formulation of histogram equalization. This added constraint preserves the mean brightness of the enhanced image. The proposed method is tested on 4 different gray scale consumer electronics images.

P. C. Wu et al. [5] proposed an enhancement which is also based on the histogram of the images. The proposed method is divided into two steps. In first step histogram of the image is divided into many sub parts with weighting mean function and in second step each sub part of histogram is piecewise equalized to achieve enhancement at local scale. The method is tested on 7 consumer electronics images. The method is objectively evaluated by peak signal to noise ratio (PSNR) and absolute mean brightness error (AMBE) measures.

B. Xu et al. [6] proposed an enhancement method in which multi level contrast stretching is performed. One is inter object contrast stretching in which structural details of images is enhanced and other is intra object contrast stretching in which textural details of image is enhanced. The method is tested on consumer electronics images.

W. T. Hsu et al. [7] proposed a method to detect the hepatocellular carcinoma (HCC) in low contrast CT images by improving its contrast. First stochastic resonance filtering is done to enhance the region of interest and then k means clustering is done and then image fusion is performed. The method is tested on 66 abdomen CT images.

M. Sajjadi et al. [8] proposed an enhancement method for brain CT images to detect cerebrovascular accidents. The proposed method designed a filter bank structure to perform the translation-invariant wavelet transform for enhancement purpose. The proposed method is tested on brain CT images.

M. Sajjadi et al. [9] proposed a method to detect early stage of ischemic stroke by doing enhancement of CT images. In proposed method non-subsampled counterlet transform is used. The method designed a simple and efficient filter for non-subsampled pyramid. The proposed method is tested on brain CT images.

M. Rudzki [10] proposed a method for automatic contrast enhancement of blood vessels in the CT images. In proposed method Frangi's vesselness filter is used to obtain the blood vessels and maximal intensity projection is used as parameter to the contrast enhancement function of the proposed method. The method is tested on the 40 liver CT images.

T. L. Tan et al. [11] proposed a method to detect brain trauma by enhancing the CT images. The method is based on histogram equalization. To preserve the mean brightness of the image first it eliminates the distribution of extreme levels and then resulting distribution is normalized and finally the transformation function is mapped to the image. The method is test on a set of CT brain images.

Z. A. Ameen et al. [12] proposed a simple and fast method to enhance the CT image. First enhancement variable is determined and then normalization is done based on size of the image. The proposed method is tested on various CT images such as abdomen, brain CT images.

V. T. An et al. [13] proposed enhancement method for CT images using image fusion. First image is detached using entropy based algorithm to produce detached image. Then decomposition wavelet transform was applied on both original and detached image for image fusion. Then inverse wavelet transform is applied to obtain final enhancement results. The method is tested on lung CT images.

H. A. Jalab and and R. W. Ibrahim [14] proposed a method for texture enhancement of medical images. The method uses fractional differential masks which are based on Srivastava-Owa fractional operators. The texture is enhanced by fractional differential based method in fractional differential spectra. Fractional power parameters are used to control the amount of enhancement in multi-fractional differential model. The method is verified by extracting the texture features. The proposed method is test on the medical images such as brain CT image.

T. Celik et al. [15] proposed an enhancement methodology based on entropy spatial distribution of the gray level pixels in the image. The spatial information of the pixels of image is obtained and then spatial distribution is calculated using its statistics of the pixels. Then uniform distribution function is mapped according to the spatial distribution of the image pixels to obtain the final enhancement results. This method is further combined with transform domain coefficients which results in global and local contrast enhancement. The method is tested on the Berkeley 500 image database.

T. K. Agarwal et al. [16] proposed a method for enhancement for medical images to improve the contrast based on histogram equalization. The method is divided into two steps. In first step histogram equalization is used for enhancement with modification in the image histogram. In second step homomorphic filter is used to sharp the image. This method is tested on mammographic images and CT images.

S. H. Malik et al. [17] applied and compared many filtering techniques to remove noise and enhancement techniques to improve the contrast of the CT images. The filters used to remove noise are mean filter, median filter, weighted median filter and wiener filter. The median filter outperforms in order to remove Gaussian noise in CT images. The enhancement methods used are histogram equalization, adaptive histogram equalization and contrast stretching. The adaptive histogram outperforms the other method in the enhancement of CT images. The experimental study is carried out on brain CT images.

Z. A. Ameen and G. Sulong [18] proposed an enhanced method that is modified version of the single scale retinex method. According to the method, the single scale retinex is first tuned, and then normalized sigmoid function is added with the parameter variation to improve its enhancement capabilities. The proposed method, tuned brightness controlled single scale retinex is tested on various CT scan images such as abdomen CT image, brain CT image.

J. J. Wang et al. [19] proposed an enhancement method that enhances the medical images by combining fuzzy contrast and non-subsampled counterlet transform. The method first low frequency components are enhanced by linear enhancement and then to deal with high frequency components adaptive threshold function is used. Then finally to enhance the global contrast fuzzy contrast is used and local details are improved by Laplace operator. The method is tested on medical images such as CT scan, MRI and digital radiographic images.

The literature of enhancement methodologies is tabularized in table 2.1. The literature related to texture feature extraction and classification is tabularized in table 2.2 and description is stated as follows:

M. Bilelloa et al. [20] proposed a method to automatically detect and classify the hypo-dense hepatic lesion using CT images. First detection of central lesion is done by intensity based histogram method and peripheral lesions are identified by liver contour refinement. The classification of lesion is done by support vector machines. The database includes 56 CT scan images with 22 simple cysts, 22 metastasis, 11 hemangiomas, and 1 is image with cyst and a hemangioma.

S. Arivazhagan et al. [21] performed texture classification using Ridglet transform and compared the classification performance with the wavelet transform. The texture features are obtained from sub bands of ridglet decomposition and these are used for classification. The database includes 20, 30,112 and 129 different images. The experimental results show that ridglet transform outperforms the wavelet transform in classification accuracy.

W. L. Zhang and X. Z. Wang [22] extracted features and perform classification of brain CT images to assist the diagnosis of tumor. Gray scale, texture, shape and symmetric features based on characteristic information of brain CT images are extracted. For classification, to build classifiers Inductive learning techniques, Radial Basis Function of Nerve Network and See5 techniques are used. The experimental results show that the proposed method assists in diagnosis for detection of disease in brain CT images.

V. S. Bharathi and L. Ganesan [23] proposed a method for selection of order for the orthogonal features. Orthogonal features such as Zernike moment and Legendre moment are calculated on the liver CT images. Then t-test based statistical feature selection method is proposed to define the order of the features. The method is applied and tested on the 50 scans of healthy liver CT images and 70 scans of abnormal liver CT images. Experimental results show that orthogonal features are effective descriptor of texture.

M. Masotti and R. Campanini [24] performed texture classification which is invariant to gray scale transformations and 90^o rotation. Firstly ranklet transform is done on images, then from resulting ranklet images texture features are extracted, then horizontal, vertical and diagonal texture features are averaged and finally classification of texture is done using support vector machine by assigning texture class to feature vector. The test data comprises of 4 sets, test data 1 contains 30, test data 2 contains 26, test data 3 contains 31 and test data 4 contains 30 images extracted from VisTex and Brodatz album.

Y. Leea et al. [25] tested the performance of different classifiers by classifying lung diseases through high resolution CT images. The classifiers used for comparison are naïve Bayesian classifier, Bayesian classifier, support vector machine and artificial neural net. The database contains CT images from 92 subjects in which 67 images of healthy lungs, 70 images with bronchiolitis obliterans, 65 images with mild centrilobular emphysema and 63 images with centrilobular Emphysema. The support vector machine outperforms the other methods in classification of lung diseases using CT images.

S. Basu et al. [26] designed a classifier model to classify lung tumors in CT images. First texture features are extracted using methods such as morphological features, co-occurrence matrix method, run length matrix, wavelet decomposition and laws features. Then feature selection is done using wrapper and relief-F methods. Then classification is performed using decision tree and support vector machines. The classification is tested on the lung CT images that contain 38 images with Adenocarcinoma and 36 images with Squamous-cell Carcinoma. The classification accuracy is 68% for classification of lung tumors in CT images with proposed model.

T. Suna et al. [27] compared the classification method support vector machine with other classifier for classification of lung cancer. The support vector machine is compared with Boosting, *k*-nearest neighbor, Decision trees, neural networks, LASSO regressions and random forests. The experiment is performed using 7438 ROI from 259 patients. Out of 7438 ROI 5984 ROIs are used to train the classifiers. The experimental result show that support vector machine outperforms the other methods in classification of benign and malignant lung cancer.

L. Devan et al. [28] proposed a method for classification of lung cancer and tuberculosis of lung using computer aided diagnosis. Texture features are extracted such as spatial gray level dependence matrix and run length matrix. Classification is done using neural network and statistical classifier. The classification is done on the 440 CT images out of which 113images are healthy, 103 images with fibrosis, 39 images with necrosis and 180 images with carcinoma. The proposed model shows classification is helpful in classifying the fibrosis and carcinoma.

Ö. Kayaaltıa et al. [29] proposed a method to classify the liver fibrosis stage in CT images which helps to avoid use of live biopsy. For classification first texture features are extracted such as gray level co-occurrence matrix, first order statistics, gray tone difference method, Laws' method, Gabor filters and Discrete Wavelet Transform. Then texture feature selection is done using sequential feature selection and exhaustive search method. Then classification is done using support vector machines and k nearest neighbor method (k-NN). Support vector machine outperforms the k-NN to some extent in classification of liver fibrosis stages.

M. Khalilinezhad et al. [30] build a model to classify the disease of the liver in 3 phase CT images. Model consists of feature extraction that includes, first order statistics, co-occurrence matrix, run length matrix, absolute gradient, auto regression model and wavelet. Then feature selection and feature reduction is done. Then classification using neural network system with optimal number or neuron in the hidden layer is designed. The database includes 40 images of liver that contains HCC tumor and 40 images with healthy liver. According to the experimental results, in first phase classification accuracy is 85%, in second phase accuracy is 95%, and in third phase also accuracy is 95%.

K. Malaa et al. [31] performed texture analysis for classification of fatty and cirrhosis liver in CT images. Bi-orthogonal wavelet based statistical features are extracted and classification is done using Probabilistic Neural Network (PNN), Back Propagation Neural Network (BPN) and Linear Vector Quantization (LVQ) Neural Network. The database includes abdomen CT images. The experimental results show that PNN outperforms the other classifier in classification of fatty and cirrhosis liver CT images.

Table 2.1 Literature review of enhancement methods

Author	**Year**	**Enhancement Method**	**database**
Y. Yu and H. Zhao	2006	Contrast limited adaptive histogram equalization	882 thoracic CT images
A.H. Mir et al.	2006	Texture feature based and fuzzy logic	100 liver CT images
I. Jafar and H. Ying	2007	Constrained variational histogram equalization	4 gray scale consumer electronic images
P. C. Wu et al.	2010	Weighting Mean-Separated Sub Histogram Equalization	7 gray scale consumer electronic images
B. Xu et al.	2010	Multi level contrast stretching: greedy iterative stretching and linear contrast stretching	gray scale consumer electronic images
W. T. Hsu et al.	2011	Stochastic resonance filtering and k mean clustering	66 abdomen CT images
M. Sajjadi et al.	2011	Translation-invariant wavelet transform	Brain CT images
M. Sajjadi et al.	2011	Non-subsampled counterlet transform	Brain CT images
M. Rudzki	2011	Frangi’s vesselness filter and maximal intensity projection	40 Liver CT images
T. L. Tan et al.	2012	Histogram equalization based extreme level elimination	Brain CT images
Z. A. Ameen et al.	2012	Image normalization based enhancement	Liver and Brain CT images
V. T. An et al.	2013	Image fusion and wavelet transform	Lung CT images
H. A. Jalab and R. W. Ibrahim	2013	Fractional differential masks based on Srivastava-Owa fractional operators	Medical images such as Brain CT images
T. Celik et al.	2014	Entropy spatial distribution	Berkeley 500 images

T. K. Agarwal et al.	2014	Histogram equalization and homomorphic filter	Mammograms and CT images
S. H. Malik et al.	2015	Mean Filter, Median Filter, Weighted Median Filter, Wiener Filter, Histogram Equalization, Adaptive Histogram Equalization And Contrast Stretching	Brain CT images
Z. A. Ameen and G. Sulong	2015	Tuned Brightness Controlled Single-Scale Retinex	Abdomen and brain CT images
J. J. Wang et al.	2015	Fuzzy contrast and Non-subsampled countelet transform	Medical images

Table 2.2 Literature review of texture feature extraction and classification methods

Author	Year	Method	Database
M. Bilelloa et al.	2004	Support vector machine	56 liver CT images
S. Arivazhagan et al.	2006	Ridglet transform	Set of 20, 30,112 and 129 different types of images
W. L. Zhang and X. Z. Wang	2007	Gray scale, texture, shape and symmetric feature extraction method. Inductive learning techniques, Radial Basis Function of Nerve Network and See5 classifiers	Brain CT images
V. S. Bharathi and L. Ganesan	2008	Orthogonal moments: Zernike moment and Legendre moment	120 liver T images
M. Masotti and R. Campanini	2008	Ranklet transform	117 images form VisTex and Brodatz album
Y. Leea et al.	2009	Naïve Bayesian classifier, Bayesian classifier, support vector machine and artificial neural net	357 CT images
S. Basu et al.	2011	morphological features, co-occurrence matrix method, run length matrix, wavelet decomposition and laws features, wrapper and relief-F methods, decision tree, support vector machine	74 lung CT images
T. Suna et al.	2013	Support vector machine, Boosting, *k*-nearest neighbor, Decision trees, neural networks, LASSO regressions and random forests	7438 ROI from 259 patients of CT images
L. Devan et al.	2014	Spatial gray level dependence matrix, run length matrix, neural network and statistical classifier	440 lung CT images
Ö. Kayaaltıa et	2014	Gray level co-occurrence matrix, first order statistics,	Liver CT images

al.		gray tone difference method, Laws' method, Gabor filters, Discrete Wavelet Transform, support vector machines and k nearest neighbor method	
M. Khalilinezhad et al.	2015	First order statistics, co-occurrence matrix, run length matrix, absolute gradient, auto regression model and wavelet, Neural network classifier	80 liver CT images
K. Malaa et al.	2015	Bi-orthogonal wavelet based statistical features, Probabilistic Neural Network (PNN), Back Propagation Neural Network (BPN) and Linear Vector Quantization (LVQ) Neural Network	Liver CT images

The literature review helped in accomplishing the present work by directing towards the way of new research. The research papers helped to understand the problems related to the proposed work.

CHAPTER 3

ENHANCEMENT OF CT IMAGES

CT images are gray scale images, so the range of pixel intensity values is from 0 to 255. So for enhancement of CT images, transformation function must be designed according to the grayscale range. In present work two spatial domain methodologies are designed for the enhancement of CT images. The enhancement methods are designed by focusing on the enhancement of textural portion of the images because characteristic information of the disease or tumor of tissue is present in the textural part of the CT images. The textural part is enhanced by applying contrast enhancement techniques. The two methods designed for enhancement of CT images are:

1. Histogram equalization with constrained variable offset

2. Modified object based contrast stretching

3.1 HISTOGRAM EQUALIZATION WITH CONSTRAINED VARIABLE OFFSET

The proposed method, histogram equalization with constrained variable offset (HECVO) is based on the basic histogram equalization. The HECVO method uses the transformation function of conventional global histogram equalization and added variable offset that preserve the global outlook of the image.

3.1.1. Background

Global histogram equalization (GHE) is most common spatial domain enhancement method. GHE enhances the global contrast of the image by varying the image histogram. The transformation function of GHE stretches the histogram bins from narrow range to full gray scale range i.e., 0 to 255. Figure 3.1 shows the histogram equalization technique, the transformation function T is applied to the histogram of original image and the intensities in histogram of enhanced image is distributed to full scale range.

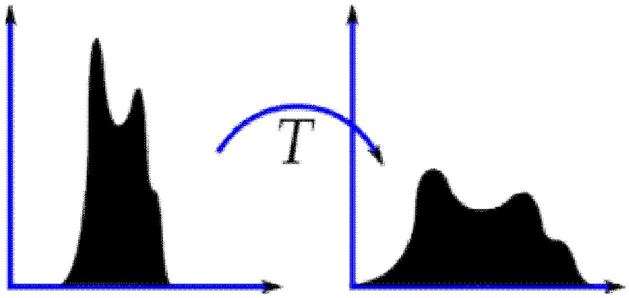

Figure 3.1 Histogram equalization [32]

Let $h_i(r)$ be normalized histogram of original image and $h_o(s)$ be normalized histogram of enhanced image, where r and s are the probability of occurrence of pixel of gray level r and s in the histogram $h_i(r)$ and $h_o(s)$ respectively. A transformation function is used to map the gray level r_x of input image to gray level s_x of output (enhanced) image [4], where r, s ϵ [0, L]:

$$s = T(r) \tag{3.1}$$

The transformation function used for image enhancement in GHE is cumulative distribution function (CDF):

$$s = T(r) = \sum_{x=0}^{r} h_i(x) \qquad for\ r = 0,1.....L \tag{3.2}$$

For gray scale images (8-bit images) L is equal to 255 [4].

Disadvantages of GHE: the main disadvantage of GHE is that it produces over enhancement artifact which causes unrealistic scenes in the images. The mean brightness of the original image gets disturbed in enhanced image, due to which global outlook of the enhanced image changes. This change in overall appearance of the image can lead to lose the detailed information present in the image.

3.1.2. HECVO method

The proposed method is designed to overcome the problem associated with GHE i.e., over enhancement artifact. HECVO method enhances the contrast of the image by using the transformation function of the conventional GHE and a constrained variable offset is added to the transformation function to preserve the mean brightness of the enhanced image [32]. The proposed method is divided into two steps:

1. Contrast enhancement using transformation function of GHE.

2. Addition of constrained variable offset to the GHE transformation function for preserving mean brightness of the image.

Step 1: To enhance the contrast of the original CT image, the transformation function of GHE is obtained using cumulative distribution function, and applied to the original image. This enhances the contrast of the image, but it changes the global outlook and mean brightness of image. Therefore, an offset is added to the transformation of GHE in second stage by taking GHE as base function.

Step 2: To preserve the global appearance of the enhanced image, mean brightness of the image should be maintained to its original range. Constrained variable offset $\Delta\lambda$ is added to the transformation of GHE to achieve the objective of preserving global appearance. According to the enhanced image brightness this variable offset is added or subtracted. If enhanced image is brighter than the original image then $\Delta\lambda$ is subtracted from the original transformation function of GHE and if the mean brightness of enhanced image is lesser than the original image then $\Delta\lambda$ is added to original transformation function of GHE, in order to sustain the mean brightness of the enhanced image closer or equal to the original image. When GHE is applied to the CT images, the mean brightness of the enhanced image is always greater than the original image. In case of CT images the offset is subtracted from the transformation function of GHE, accordingly new transformation function is as follows:

$$T(r) = \sum_{x=0}^{r} h_i(x) - \Delta\lambda \qquad (3.3)$$

where $\Delta\lambda$ is constrained variable offset, it controls the over enhancement produced by the GHE. The offset is constrained variable because it varies according to the histogram values of original image and it limits the enhancement from producing undesirable saturation artifacts and over stretching of histogram. The constrained variable offset is calculated as follows:

$$\Delta\lambda = |k| - \left(\frac{|k|}{L+1} \times x \right) \tag{3.4}$$

where x represents the bin value of gray scale of histogram of the original image and k is a constant which is calculated iteratively according to the difference of mean brightness between original and enhanced image. The value of constant k is initially set to any arbitrary value, say $k = 1$, then transformation function given in Eq.(3.3) is applied and the mean brightness difference ΔM is calculated. The value of k is increased or decreased iteratively according to the mean brightness difference of enhanced image, till the mean brightness difference is minimized to a tolerable range. The Mathematical formulation for mean brightness difference is shown in Eq. (3.5).

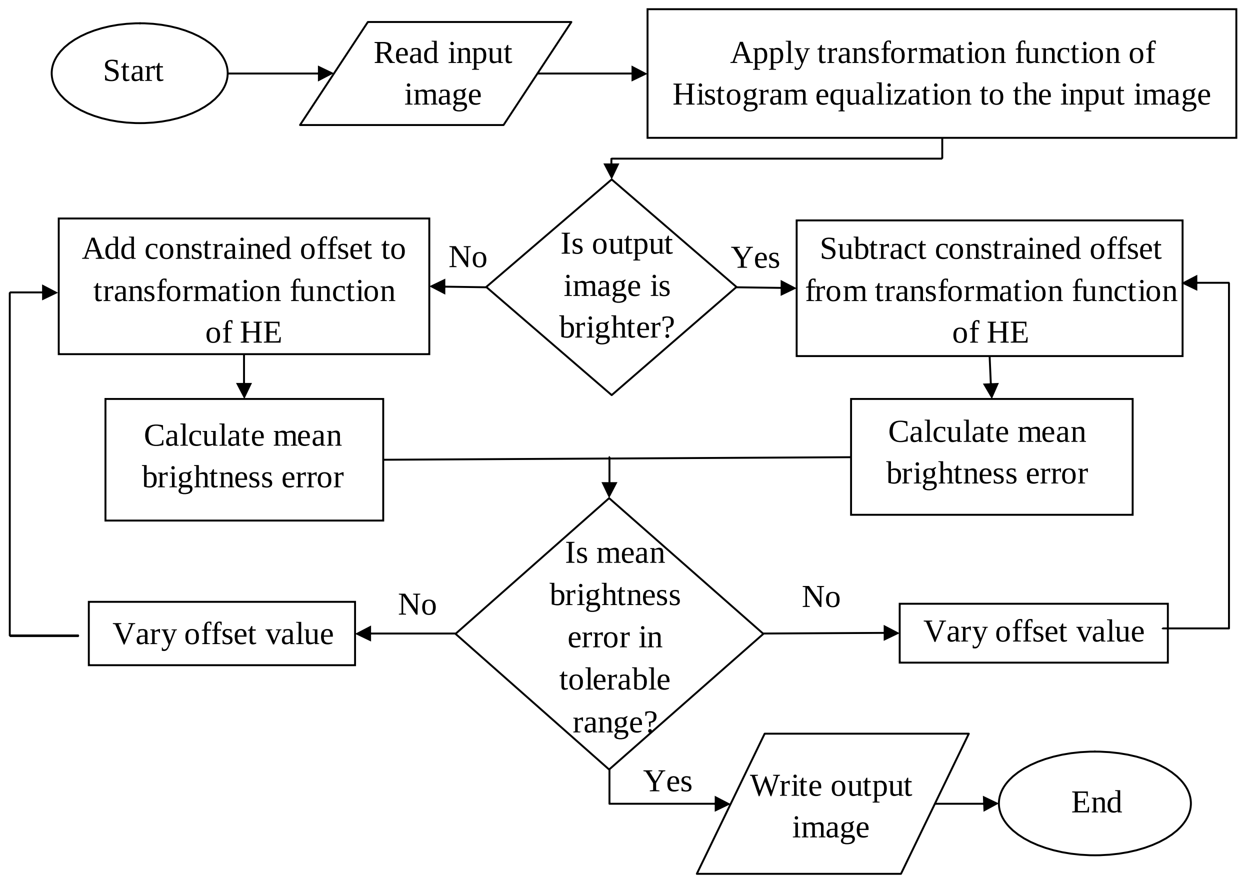

Figure 3.2 Flow chart of HECVO method

$$\Delta M = \frac{\left(\sum_{x=0}^{r} x \times h_i(x) - \sum_{x=0}^{r} T(r) \times h_i(x) \right)}{m \times n} \tag{3.5}$$

where $m \times n$ is size of the original image.

The proposed HECVO method enhances the contrast of the CT images by controlling the over stretching of histogram and preserving the mean brightness of the original image in enhanced image. The flowchart explaining the key steps of HECVO method is shown in figure 3.2.

3.2 MODIFIED OBJECT BASED CONTRAST STRETCHING

Modified object based contrast stretching (MOBCS) method is designed to mainly enhance the texture portion of the CT images. MOBCS method is proposed by modifying the object based multilevel contrast stretching method of B. Xu and Y. Zhuang (IEEE Transaction on Consumer Electronics 3:1746-1754, 2010). MOBCS is not a global approach, it enhances the texture of the CT images using local approach of enhancement.

3.2.1. Background

The basic methods and definitions used in the proposed method are explained in this section.

Morphological watershed method is a segmentation technique in which the image is visualized as a topographic relief, where intensities of pixels represent the altitude of the relief map. Imagine the topographic relief is flooded through water from the bottom of the catchment basin. When water is about to reach the top of the relief and two catchment basins are about to merge then a dam is constructed. These constructed dams are known as watershed lines. These watershed lines are the required segmentation [33]. Morphological watershed segmentation is used in proposed method for segmentation of image. Watershed method is very sensitive to the edges present in the image, so this method over segments the regions in the image. To prevent the over segmentation produced by watershed is reduced by applying gradient thresholding. This gradient thresholding is applied before applying the watershed segmentation, so it is the pre-processing method. The gradient thresholding is applied to the gradient image and gradient map obtained after thresholding is passed to the watershed segmentation. Gradient thresholding is implemented by first obtaining gradient map using sobel operator; sobel operator is quite stable operator [33]. Mathematical formula for obtaining gradient map is as follows:

$$G(x,y) = |G_x(x,y)| + |G_y(x,y)| \tag{3.6}$$

where $G(x,y)$ is gradient magnitude map, $G_x(x,y)$ and $G_y(x,y)$ magnitudes in x direction and y direction respectively. The gradient thresholding is implemented as follows:

$$G_i(x,y) = \begin{cases} G_t & if\ G(x,y) < G_t \\ G(x,y) & otherwise \end{cases} \tag{3.7}$$

where G_t is gradient threshold and G_i is new gradient magnitude map after thresholding.

Watershed segmentation results obtained after gradient thresholding still contains some over segmentation. To prevent further segmentation produced by watershed method post-processing is applied, i.e., region merging. Region merging is a method that merges the pair of adjacent regions produced after the segmentation to reduce the amount of segmented regions. The performance of the region merging depends on the merging criteria. Merging criteria defines how the regions get merged. Some common merging criteria proposed in literature are Ward criterion, mean criterion, just noticeable difference criterion, ward-mean criterion, linear luminance criterion, border criterion etc. each merging criteria have its own dissimilarity function. Region merging is applied by first obtaining the adjacent regions according to the merging criteria, and then the dissimilarity function is minimized according to the adjacent regions obtained from the image [6]. The dissimilarity function is minimized till it reaches a specified stopping condition. The stopping condition can be decided by estimated standard deviation of noise. The estimated standard deviation of noise is calculated by first filtering the image to reduce the noise and calculating the standard deviation between original image and filtered image.

Another methodology used in proposed method is greedy iterative stretching [34]. Greedy iterative method is a contrast stretching method. This is an iterative method in which the image is imagined as a mesh and the pixel intensities are assumed as height of mesh. For each iteration a threshold plane for the mesh is decided and the connected components are calculated which have intensities above the threshold plane. These connected components calculated for each iteration are known as hillocks. These hillocks are scaled according to specified constrained; constraints prevent the saturation in stretching. After scaling the hillocks for one threshold plane, the threshold plane is swept above for further stretching. This sweeping of threshold plane and scaling of hillocks is done iteratively between the lower and upper limit decided. Mostly the lower limit is 0 i.e., the lower value of gray scale range and upper limit is 255 which is the upper value of gray scale range. For full scale stretching the image is inverted and then again greedy iterative stretching method is applied to inverted image in the same manner. After enhancement the image is again inverted to get back the final enhanced image. Figure 3.3 shows the graphs showing key steps of the greedy iterative stretching if applied to the one dimensional (1D) signal.

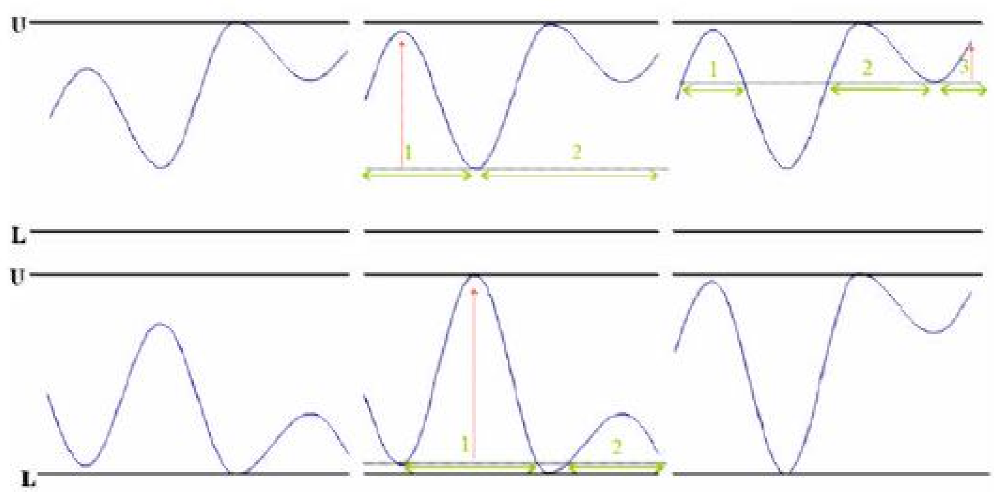

Figure 3.3 Graphs showing the steps of greedy iterative stretching when applied to 1D signal. [34]

3.2.2. Object based multilevel contrast stretching

Object based multilevel contrast stretching (OBMCS) method is proposed by Xu and Zhuang in 2010 [6]. This method is applied on the consumer electronics images and enhanced results are obtained. OBMCS method performs multilevel contrast stretching, one contrast is stretched at inter-object level and another contrast is stretched at intra-object level. The inter-object contrast stretching leads to structural enhancement in image and the intra-object contrast stretching enhances the textural portion of the image. First the gradient magnitude map $G(x, y)$ is calculated for the input image $I(x, y)$ using sobel operator. Then gradient thresholding is applied to the gradient map. The new gradient map $G_i(x, y)$ is obtained after thresholding as explained in Eq. (3.7). Watershed segmentation method is applied to the thresholded gradient map. To prevent over segmentation post processing i.e., region merging is applied to the segmented image. The merging criterion used for the region merging is mean criterion. The dissimilarity function for the mean criterion of merging is:

$$\delta(S_a, S_b) = |\mu(S_a) - \mu(S_b)| \tag{3.8}$$

Where $\mu(S)$ denotes the mean of region S. The merging process is continued till it reaches the stopping condition δ_T. After segmentation process the image is divided into two parts based on segmented image. One part is object approximation image (OAI) and another part is object error image (OEI). Object approximation image is obtained by taking the mean of all pixel values present in a region and replacing all the pixel values by that mean value in the region of the image. OEI is obtained by subtracting the OAI from the original image. The OAI and OEI are calculated as given in Eq. (3.9) and (3.10) respectively:

$$I_{OAI}(x, y) = \mu(S_{(x,y)}) \tag{3.9}$$

$$I_{OEI}(x, y) = I(x, y) - I_{OAI}(x, y) \tag{3.10}$$

The original image can be obviously obtained again as follows:

$$I(x, y) = I_{OAI}(x, y) + I_{OEI}(x, y) \tag{3.11}$$

Object approximation image is enhanced by applying greedy iterative stretching and this enhancement is known as inter-object contrast stretching. Object error image is enhanced by linear stretching and it is known as intra-object contrast stretching. After enhancement of both the images separately, they are added to obtain the final enhanced image.

3.2.3. Proposed method

The proposed method is modified version of OBMCS method. Some modifications have been made to formulate the method suitable for the enhancement of CT images. By modifications in OBMCS method modified object based contrast stretching (MOBCS) method is designed. CT images have good global contrast and exhibit high quality structural details. So there is no need to improve the structural part of the CT images. In MOBCS method the main focus is enhancement of textural portion in the CT images. The proposed method is divided into three steps:

- Segmentation of image using watershed segmentation method.
- Intra-object contrast stretching.
- Mean adjustment in image.

In first step, segmentation is applied to the input image. Morphological watershed segmentation is applied with pre and post processing steps as similar to the OBMCS method i.e., gradient thresholding as pre processing and region merging as post processing. The change is made to the merging criterion of the region merging. Ward criterion is used as merging criterion in proposed method. The dissimilarity function for ward criterion is as follows:

$$\delta(S_a, S_b) = \frac{\|S_a\| \cdot \|S_b\|}{\|S_a\| + \|S_b\|}\left[\mu(S_a) - \mu(S_b)\right]^2 \tag{3.12}$$

where $\|S\|$ is the number of pixels in region S. Ward criterion is used in MOBCS method instead of mean criterion because ward criterion is superior to mean criterion. Ward criterion tends to minimize the total error introduced due to merging between adjacent regions of the segmented image. Ward criteria does not merge only small regions but it take care about the region homogeneity. It also eliminates double edges and removes noise.

In second step, object approximation image and object error image is calculated as explained in Eq. (3.9) and (3.10) respectively. In MOBCS method only intra-object stretching is done because enhancement of CT image is focused mainly on texture portion. Intra-object stretching leads to textural improvement in the image. Intra object stretching is done by applying greedy iterative stretching method on OEI, which is explained in section 3.2.1. Greedy iterative method is applied with the following constraints:

$$1 \le \frac{I'(x,y) - \mu'(S_{(x,y)})}{I(x,y) - \mu(S_{(x,y)})} \le (1+\lambda) \tag{3.13}$$

$$L \le I'(x,y) \le U \tag{3.14}$$

where $I'(x,y)$ is enhanced result of original image $I(x,y)$, $\mu'(S_{(x,y)})$ is mean of region S of enhanced image and $\mu(S_{(x,y)})$ is mean of region S of original image. λ is the variable that controls the amount of stretching in the enhancement process. L and U are the lower and upper limit for the sweeping of threshold plane. Generally, lower limit is 0 and upper limit is 255 which is the range of grayscale levels. After applying greedy iterative method on OEI, the image is inverted and then again greedy iterative method is applied to inverted image. Image is again inverted to obtain the final enhancement result of OEI $I'_{OEI}(x,y)$. Enhancement of OAI is not done in this method.

In third step, mean brightness adjustments are made to the enhanced results obtained after intra-object stretching. Mean adjustment is required because additional result of enhanced OEI with original OAI cause overall brightness increment. This brightness increment causes disturbance in the visibility of details present in the image. To reduce the brightness, mean brightness adjustments are made. Before adding the enhanced OEI with original OAI, some percentage of mean of brightness of enhanced OEI is added to the enhanced OEI and the same amount of percentage of mean brightness of OAI is reduced from OAI. This represented as follows:

$$NI'_{OEI}(x,y) = I'_{OEI}(x,y) + \alpha\%\ of\ \mu(I'_{OEI}(x,y)) \tag{3.15}$$

$$NI_{OAI}(x,y) = I_{OAI}(x,y) - \alpha\%\ of\ \mu(I_{OAI}(x,y)) \tag{3.16}$$

where α is a variable that decides the amount of brightness change. The final enhanced image is obtained as follows:

$$E(x,y) = NI'_{OEI}(x,y) + NI_{OAI}(x,y) \tag{3.17}$$

Block diagram of key steps of MOBCS method is shown in figure 3.4.

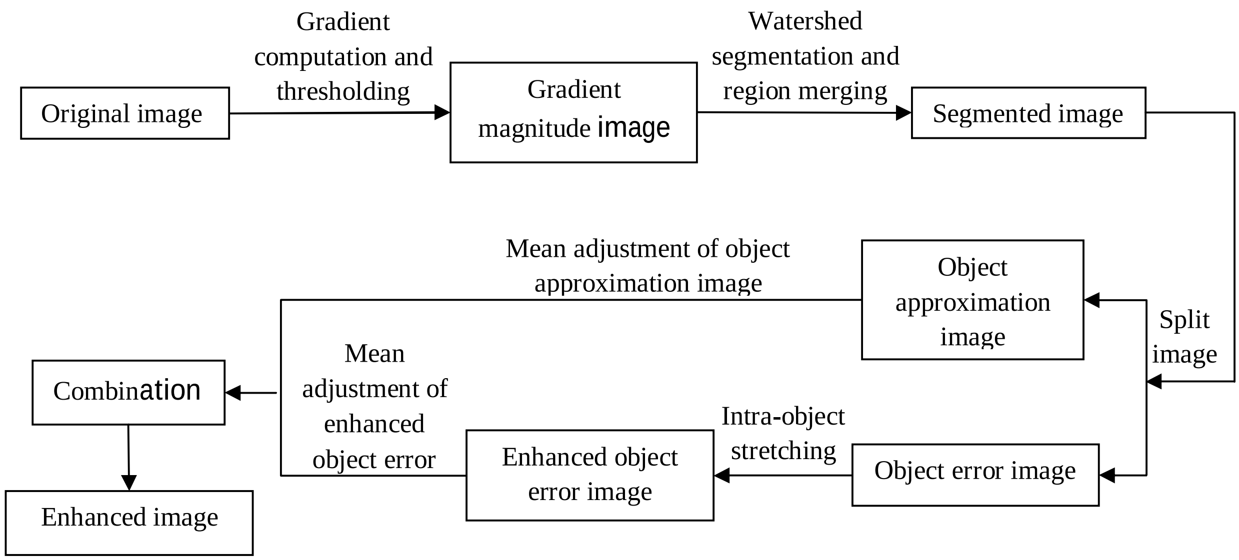

Figure 3.4 Block diagram of MOBCS method

The two enhancement methodologies are proposed and applied to CT images to obtain the enhanced images such that it help in better diagnosis of disease by both visual inspection and computer aided diagnosis system. The results obtained by the both enhancement methodologies are given for further processing such as texture feature extraction and classification model. This is explained in further chapters.

CHAPTER 4

TEXTURE FEATURE EXTRACTION AND ANALYSIS

The texture of the image gives information of the spatial arrangement of the intensities present in the image. Texture of the image assists in extraction of useful details. Texture analysis is very useful in medical image processing. It helps to classify the tumor or disease in the medical images such as CT images. Texture analysis can be done calculating texture features of the images. There are basically three approaches that represent image texture:

- Statistical method: according to this approach image texture is the quantitative measure of the arrangement of the intensities of the image.
- Structural method: according to this approach image texture is representation of pre-defined structures or primitive texels that are in periodic patterns.
- Spectral method: according to this approach image texture is representation of the frequency components of the image, which can be defined by Fourier transform or wavelet transform.

Statistical method is easy to calculate for texture analysis because it is the variation or arrangement of spatial intensity of image. According to the statistical approach texture features are calculated which are the mathematical representation of texture.

4.1. TEXTURE FEATURES

Texture features are extracted to obtain the useful information from the CT images. These texture features helps to verify the enhancement methodology is helpful in enhancement of texture of the images. Texture features are further used in the classification of the normal and abnormal tissue. In present work following texture features are extracted from the CT images:

- First order statistics (FOS)
- Gray Level Co-occurrence Matrix (GLCM)
- Gray Level Run Length Matrix (GLRLM)
- Gray Tone Difference Matrix (GTDM)
- Hu moments (HUM)
- Zernike moments

- Gabor features
- Other statistical features

4.1.1. First order statistics (FOS)

First order statistics (FOS) calculates the features based on the first order statistic of the image pixels without considering relationship of neighborhood of pixels [28]. The mathematical formulations of FOS features are as follows:

$$Mean\ (\mu) = \frac{1}{M \times N} \sum_{a=1}^{M} \sum_{b=1}^{N} I(a,b) \tag{4.1}$$

$$Variance\ (\sigma^2) = \left[\frac{1}{M \times N} \sum_{a=1}^{M} \sum_{b=1}^{N} (I(a,b) - \mu)^2 \right] \tag{4.2}$$

$$Energy = \frac{1}{M \times N} \sum_{a=1}^{M} \sum_{b=1}^{N} I^2(a,b) \tag{4.3}$$

$$Skewness = \frac{1}{M \times N \times \sigma} \sum_{a=1}^{M} \sum_{b=1}^{N} (I(a,b) - \mu)^3 \tag{4.4}$$

$$Kurtosis = \frac{1}{M \times N \times \sigma^2} \sum_{a=1}^{M} \sum_{b=1}^{N} (I(a,b) - \mu)^4 - 3 \tag{4.5}$$

4.1.2. Gray Level Co-occurrence Matrix (GLCM)

Gray Level Co-occurrence Matrix (GLCM) is one of the most popular techniques for extraction of texture features. GLCM shows the relation between the neighboring pixels and occurrence frequency of intensity levels at specified distance and orientation. The distribution of occurrence of a pair of gray level values (a,b) reflects the GLCM matrix P(a,b|e,θ), where e is the inter-sample distance and θ is the direction. Normally θ= {0º, 45º, 90º, 135º} [28]. Features calculated for GLCM is described with their mathematical formula as follows:

$$Angular\ second\ moment\ \ f_1 = \sum_a \sum_b \{P(a,b)\}^2 \tag{4.6}$$

$$Contrast\ \ f_2 = \sum_{q=0}^{R-1} q^2 \left\{ \begin{matrix} \sum_{a=1}^{R} \sum_{b=1}^{R} P(a,b) \\ |a-b| = q \end{matrix} \right\} \tag{4.7}$$

$$Correlation\ f_3 = \frac{\sum_a \sum_b (a,b)P(a,b) - \mu_x \mu_y}{\sigma_x \sigma_y} \tag{4.8}$$

$$Sum\,of\ squares\ \ f_4 = \sum_a \sum_b (a-\mu)^2 P(a,b) \tag{4.9}$$

$$Inverse\ \ Difference\,Moment\ \ f_5 = \sum_a \sum_b \frac{1}{1+(a-b)^2} P(a,b) \tag{4.10}$$

$$Sum\ Average\ \ f_6 = \sum_{a=2}^{2R} aP_{x+y}(a) \tag{4.11}$$

$$Sum\,Variance\ f_7 = f(j,l) \tag{4.12}$$

$$Sum\ Entropy\ \ f_8 = -\sum_{a=2}^{2R} P_{x+y}(a)\log(P_{x+y}(a)) \tag{4.13}$$

$$Entropy\ \ f_9 = -\sum_a \sum_b P(a,b)\log(P(a,b)) \tag{4.14}$$

$$Difference\,Variance\ \ f_{10} = Variance\ of\ \ P_{x-y} \tag{4.15}$$

$$Difference\,Entropy\ \ f_{11} = \sum_{a=0}^{R-1} P_{x-y}(a)\log\{P_{x-y}(a)\} \tag{4.16}$$

Information measure of correlation

$$f_{12} = \frac{\left[-\sum_a \sum_b P(a,b)\log(P(a,b))\right] - \left[-\sum_a \sum_b P(a,b)\log(P_x(a)P_y(b))\right]}{\max\left[\left[-\sum_a \sum_b P(a,b)\log(P(a,b))\right], \left[-\sum_a \sum_b P(a,b)\log(P_x(a)P_y(b))\right]\right]}$$

$$f_{13} = \left(1-\exp\left[-2.0\left(\left[-\sum_a \sum_b P_x(a)P_y(b)\log(P_x(a)P_y(b))\right] - \left[-\sum_a \sum_b P(a,b)\log(P_x(a)P_y(b))\right]\right)\right]\right)^{\frac{1}{2}} \tag{4.17}$$

Where R is the number of gray levels in the image, $\mu_x, \mu_y, \sigma_x, \sigma_y$ are mean and standard deviation of P_x, P_y respectively.

4.1.3. Gray Level Run Length Matrix (GLRLM)

Gray level run length matrix (GLRLM) is the feature extraction method which extracts the second order statistic from the image. The set of sequential gray level pixels that are same and have same direction forms the gray level run. The run length is the number of pixels and run length value is the frequency of occurrence of runs in the image. GLRLM is a matrix P(a,b|θ) where a is the number of runs in the b length in the θ direction [28]. The mathematical formulation of texture features of GLRLM is shown in Eq.(4.18) to Eq.(4.28).

$$Short\ Run\ Emphasis\ (SRE) = \frac{1}{K}\sum_{a=1}^{M}\sum_{b=1}^{N}\frac{P(a,b)}{b^2} \tag{4.18}$$

$$Long\ Run\ Emphasis\ (LRE) = \frac{1}{K}\sum_{a=1}^{M}\sum_{b=1}^{N}P(a,b)b^2 \tag{4.19}$$

$$Gray-Level\ Nonuniformiy\ (GLN) = \frac{1}{K}\sum_{a=1}^{M}\left(\sum_{b=1}^{N}P(a,b)\right)^2 \tag{4.20}$$

$$Run\ Length\ Nonuniformity\ (RLN) = \frac{1}{K}\sum_{b=1}^{N}\left(\sum_{a=1}^{M}P(i,j)\right)^2 \tag{4.21}$$

$$Run\ Percentage\ (RP) = \frac{1}{n}\sum_{b=1}^{N}\sum_{a=1}^{M}P(a,b) \tag{4.22}$$

$$Low\ Gray-Level\ Run\ Emphasis\ (LGRE) = \frac{1}{K}\sum_{a=1}^{M}\sum_{b=1}^{N}\frac{P(a,b)}{b^2} \tag{4.23}$$

$$High\ Gray-Level\ Run\ Emphasis\ (HGRE) = \frac{1}{K}\sum_{a=1}^{M}\sum_{B}^{N}P(a,b)b^2 \tag{4.24}$$

$$Short\ Run\ Low\ Gray-Level\ Emphasis\ (SRLGE) = \frac{1}{K}\sum_{a=1}^{M}\sum_{b=1}^{N}\frac{P(a,b)}{a^2b^2} \tag{4.25}$$

$$Short\ Run\ High\ Gray-Level\ Emphasis\ (SRHGE) = \frac{1}{K}\sum_{a=1}^{M}\sum_{b=1}^{N}\frac{P(a,b)a^2}{b^2} \tag{4.26}$$

$$Long\ Run\ Low\ Gray-Level\ Run\ Emphasis\ (LRLGE)=\frac{1}{K}\sum_{a=1}^{M}\sum_{b=1}^{N}\frac{P(a,b)b^2}{a^2} \tag{4.27}$$

$$Long\ Run\ High\ Gray-Level\ Run\ Emphasis\ (LRHGE)=\frac{1}{K}\sum_{a=1}^{M}\sum_{b=1}^{N}P(a,b)a^2 \tag{4.28}$$

where K and n are total number of runs and total number of pixels in the image respectively.

4.1.4. Gray Tone Difference Matrix (GTDM)

Gray tone difference matrix (GTDM) is a column matrix which is used for further feature extraction [28]. The mathematical formula for the features of GTDM is shown in Eq.(4.24) to Eq.(4.28).

$$Coarseness\ C_1=\left(\varepsilon+\sum_{a=0}^{R}P_aZ(a)\right)^{-1},\quad P_i=\frac{N_a}{n^2} \tag{4.29}$$

$$Contrast\ C_2=\left[\frac{1}{N_k(N_k-1)}\sum_{a=0}^{R}\sum_{b=0}^{R}P_aP_b(a-b)^2\right]\left[\left(\frac{1}{n^2}\sum_{a=}^{R}Z(a)\right)\right] \tag{4.30}$$

$$Busyness\ C_3=\frac{\sum_{a=0}^{R}P_aZ(a)}{\sum_{a=0}^{R}\sum_{b=0}^{R}\left|aP_a-bP_b\right|},\quad P_a\neq 0, P_b\neq 0 \tag{4.31}$$

$$Complexity\ C_4=\sum_{a=0}^{R}\sum_{b=0}^{R}\frac{|a-b|}{n^2(P_a+P_b)}\left[P_aZ(a)+P_bZ(b)\right],\quad P_a\neq 0, P_b\neq 0 \tag{4.32}$$

$$Strength\ C_5=\frac{\sum_{a=0}^{R}\sum_{b=0}^{R}(P_a+P_b)(a-b)^2}{\varepsilon+\sum_{a=0}^{R}Z(a)},\quad P_a\neq 0, P_b\neq 0 \tag{4.32}$$

where R is the highest gray tone value, N_k is total number of different gray values in the image. $Z(a)$ is the GTDM value at a level.

4.1.5. Hu Moments

There are seven moment invariants which are invariant of rotation obtained from geometric moments. These moments are known as Hu moments [33]. The mathematical formulation of these seven moment invariants are as follows:

$$H_1 = (\upsilon_{20} + \upsilon_{02}) \tag{4.34}$$

$$H_2 = (\upsilon_{20} - \upsilon_{02})^2 + 4\upsilon_{11} \tag{4.35}$$

$$H_3 = (\upsilon_{30} - 3\upsilon_{12})^2 + (3\upsilon_{21} - \upsilon_{03})^2 \tag{4.36}$$

$$H_4 = (\upsilon_{30} + \upsilon_{12})^2 + (\upsilon_{21} + \upsilon_{03})^2 \tag{4.37}$$

$$H_5 = (\upsilon_{30} - 3\upsilon_{12})^2 (\upsilon_{30} + \upsilon_{12})\left[(\upsilon_{30} + \upsilon_{12})^2 - 3(\upsilon_{21} + \upsilon_{12})^2\right] \tag{4.38}$$

$$\begin{aligned} H_6 = (\upsilon_{20} - \upsilon_{02})\left[(\upsilon_{30} + \upsilon_{12})^2 - (\upsilon_{21} + \upsilon_{03})^2\right] + 4\upsilon_{11}(\upsilon_{30} + \upsilon_{12})(\upsilon_{21} + \upsilon_{03}) + (3\upsilon_{21} - \upsilon_{03})(\upsilon_{21} + \upsilon_{03}) \\ \left[3(\upsilon_{30} + \upsilon_{12})^2 - (\upsilon_{21} + \upsilon_{03})^2\right] \end{aligned} \tag{4.39}$$

$$\begin{aligned} H_7 = (3\upsilon_{21} - \upsilon_{03})(\upsilon_{30} + \upsilon_{12})\left[(\upsilon_{30} + \upsilon_{12})^2 - 3(\upsilon_{21} - \upsilon_{03})^2\right] - (\upsilon_{30} + 3\upsilon_{12})(\upsilon_{21} + \upsilon_{03}) \\ \left[3(\upsilon_{30} + \upsilon_{12})^2 - (\upsilon_{21} + \upsilon_{03})^2\right] \end{aligned} \tag{4.40}$$

where υ_{pq} is normalized central geometric moments.

4.1.6. Zernike Moments

Zernike moments include set of complex polynomials which describe the shape features [23]. The set of polynomials form the complete set interior to the unit circle. The polynomials are defined as follows:

$$V_{ef}(x, y) = R_{ef}(x, y) \exp\left[jf \tan^{-1}(y/x) \right] \tag{4.41}$$

Where e is the order and f is the repetition for digital image function. The radial polynomial is represented as follows:

$$R_{ef}(x, y) = \frac{\sum_{a=0}^{e-|f|/2} -1^a (x^2 + y^2)^{(e/2)-a} (e-a)!}{a!\left(\frac{e+|f|}{2} - a\right)!\left(\left(\frac{e-|f|}{2} - a\right)!\right)} \tag{4.42}$$

4.1.7. Gabor features

Gabor features are extracted by first calculating Gabor filter bank and then convoluting this filter with the image [28]. The Gabor filters can be obtained as follows:

$$Gf(x,y,\vartheta,\theta)=\exp\left[-\frac{1}{2}\left(\left(x'/s_{x'}\right)^2+\left(y'/s_{y'}\right)^2\right)\right]\cos(2\pi\vartheta x) \tag{4.43}$$

$$x'=x\cos(\theta)+y\sin(\theta),\quad y'=y\cos(\theta)+x\sin(\theta)$$

Where $s_{x'}$ and $s_{y'}$ are the variance in the direction of x' and y' respectively. ϑ is the frequency and θ is the orientation. This filter is convolved with the image $I(x,y)$ then an filtered output image is obtained i.e., $Op(x,y,\theta,s_{x'},s_{y'})$. The output obtained after convolution is average to obtain single texture feature that is shown as follows:

$$tx(\theta,s_{x'},s_{y'})=\sum_x\sum_y Op(x,y,\theta,s_x,s_y) \tag{4.44}$$

4.1.8. Other statistical features

There are two other statistical features, periodicity and roughness [35]. Periodicity and roughness are generated by three statistical feature matrices under the maximum inter sample distance. These three matrices are shown as follows:

$$Contrast\ Matrix\ con(\Delta i,\Delta j)=Ex\left[(Gl(i+\Delta i,j+\Delta j)-Gl(i,j))^2\right] \tag{4.45}$$

$$Co\,\mathrm{var}\,iance\ Matrix\ \mathrm{cov}(\Delta i,\Delta j)=Ex\left[(Gl(i+\Delta i,j+\Delta j)-\mu)(Gl(i,j)-\mu)\right] \tag{4.46}$$

$$Dissimilarity\ Matrix\ dss(\Delta i,\Delta j)=Ex\left[|\,Gl(i+\Delta i,j+\Delta j)-G(i,j\,|\right] \tag{4.47}$$

Where $Ex[\cdot]$ is the expectation operation, $(\Delta i,\Delta j)$ is inter sample distance, $Gl(i,j)$ is the gray level at pixel (i,j), μ is the mean of pixel values of image.

4.2. FEATURE SELECTION

Feature selection is done by two methods in present work. One method is box plot study and another method is sequential feature selection method. First box plot study is conducted to check whether the features are eligible for classification or not. Box plot for each feature is designed for two class normal and abnormal tissue of CT image. Then by visual inspection those features are selected in which distribution of data shows sufficient inter class difference. After box plot study, sequential feature selection (SFS) method is applied to the selected features to reduce redundancy and over fitting in the feature data [36]. There are basically two components of SFS:

- Selection criterion: the criterion tends to minimize the feature set and define when to stop minimizing it. The common criterion for feature selection is misclassification rate.
- Sequential search algorithm: this defines how the features are selected while taking criterion into consideration.

There are two variants of SFS:

- Sequential forward selection: this selection process adds features to an empty set till the further addition of feature does not decrease the criterion.
- Sequential backward selection: this selection process removes the features from the full set of features till the further removal of feature does not increase the criterion.

After texture feature extraction and selection of features, the selected features are used for classification purpose to categorize the normal and abnormal tissue.

CHAPTER 5

CLASSIFICATION

Classification is the process in which ideas and objects are categorized in different classes. Recognition and differentiation can also referred as classification. Classification is considered as an example of supervised learning, in the terminology of machine learning. It is done on the basis of training set of data that contains the observations (or features) whose membership to the categories is known. Training set of data assists in differentiation of test data into different categories. These categories or classes are determined by the training set. Classification is basically thought as two different problems:

- Binary classification: this type of classification includes only two classes, in which data is categorized.
- Multiclass classification: this type of classification includes more than two classes, in which data is categorized.

The algorithm that classifies the data set into classes is known as classifier. There are many classification algorithms such as decision trees, ensembles (bagging, boosting, random forest), k-nn, linear regression, naive bayes, neural networks, logistic regression, perceptron, support vector machine (SVM) and relevance vector machine (RVM). In the present work, support vector machine (SVM) algorithm is used for classification.

Classification result is generally shown in the form of confusion matrix. Confusion matrix is a contingency table that shows the performance of the classification. The example of confusion matrix is shown in table 5.1, where TP is true positive, TN is true negative, FP is false positive and FN is false negative.

Table 5.1 Example of confusion matrix

		Predicted class	
		Yes	No
Actual class	Yes	TP	FN
	No	FP	TN

The most common parameters of performance of classification are accuracy, sensitivity, specificity. These are calculated from the confusion matrix as follows:

$$Accuracy = \frac{TP + TN}{TP + TN + FP + FN} \tag{5.1}$$

$$Sensitivity = \frac{TP}{TP + FN} \tag{5.2}$$

$$Specificity = \frac{TN}{TN + FP} \tag{5.3}$$

5.1 SUPPORT VECTOR MACHINE

Support vector machine is supervised learning model with related learning techniques that evaluate data and identify patterns, used for classification [27]. SVM is basically a linear classifier but it can also perform non-linear classification. SVM model is designed by taking training set whose classes are known by separating this known data into their individual classes. This model is representation of observations as points in a space and it is used to classify the new unknown or test data into same classes by separating them with visible gap in the space. SVM construct a set of hyper planes in the infinite or high dimensional space that is used for classification. For good separation this hyper plane must have maximum possible distance from the nearest training data point of all classes in the space. This means that larger the margin, lower the error of classifier. Margin means the maximum distance between the lines parallel to the hyper plane that contains no interior data points. In real, finite dimensional space is used instead of high dimensional space because in high dimensional space it is difficult to separate the data due to the non linearity of the data set. Figure 5.1 shows the classification of two classes, one is '+' (positive) class and other is '-' (negative) class.

Support vectors are the data points which nearest to the hyper plane. When the data points are represented as p-dimensional feature vector and if classifier separates the set of data into two classes with (p-1) dimensional hyperplane then it is known as linear classifier. There can be many hyperplanes to separate the data, the best hyper plane is chosen with maximum margin and this is known as maximum margin hyperplane. The linear classifier that defines it is known as maximum margin classifier.

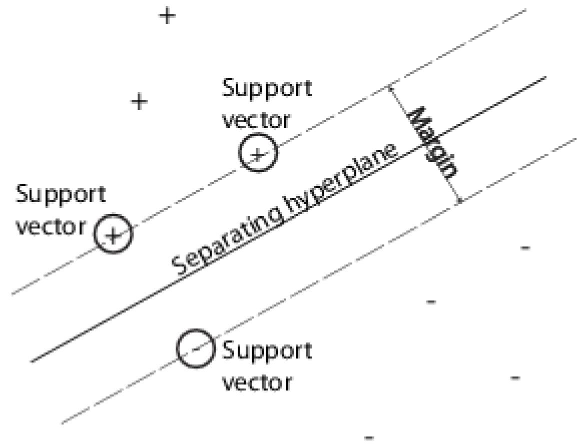

Figure 5.1 Classification using SVM [37]

The mathematical formulation of linear SVM classifier is explained in this section.

Let training data T_r is known, it is a set of z points of the form:

$$T_r = \{(X_i, Y_i) \mid X_i \in R^p, Y_i \in \{-1,1\}\}_{i=1}^{z} \tag{5.4}$$

where X_i is a real vector of p dimension, Y_i defines to which class X_i belongs i.e, 1 or -1. The separating hyper plane will decide to which class the X_i belongs. The hyper plane for set of point satisfies the following equation:

$$W \bullet X - d = 0 \tag{5.5}$$

where W is a normal vector to hyperplane, $\bullet$ represents the dot product. The offset of the hyperplane along the W from the origin is defined by the parameter $\frac{b}{\|W\|}$. Two hyperplanes can be selected if training data is linearly separable. The hyperplanes are selected such that there exists no data points between two hyperplanes, and the region between them is known as margin. These hyperplanes are as follows:

$$W \bullet X - d = 1 \tag{5.6}$$

and

$$W \bullet X - d = -1 \tag{5.7}$$

The distance between two hyperplanes is $\frac{2}{\|W\|}$. To maximize the margin $\|W\|$ must be minimized.

Following constraint also must be added to prevent the data points to fall in the margin:

$$Y_i(W \bullet X_i - d) \geq 1, \quad \text{for all } 1 \leq i \leq z \tag{5.8}$$

Following optimization problem is created according to the above discussion:

$$\begin{aligned} &\text{Minimize } \|\mathrm{W}\| \\ &\text{Subject to: } \mathrm{Y_i}(W \bullet X_i - d) \geq 1 \end{aligned} \tag{5.9}$$

Training of classes with maximum margin hyperplane is shown in figure 5.2.

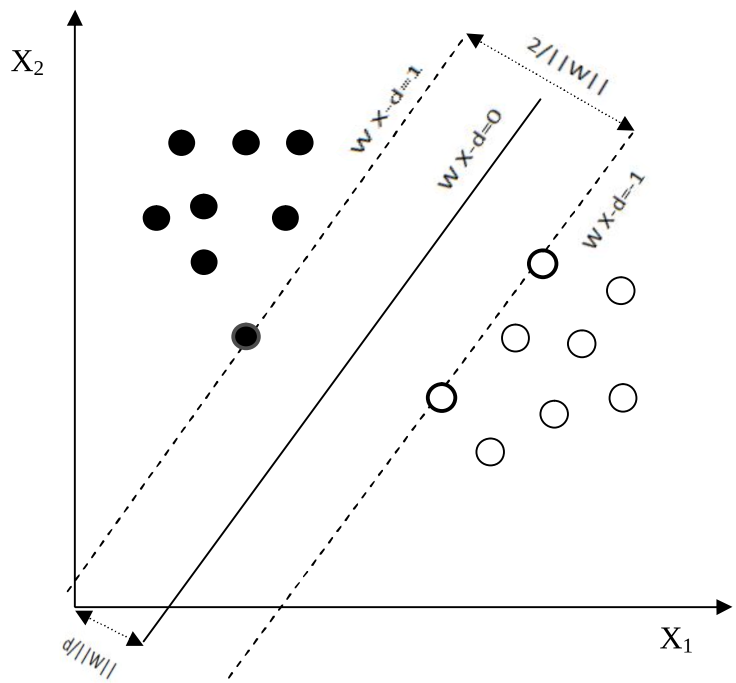

Figure 5.2 SVM training with samples of two classes.

5.1.1. Primal form

The optimization problem formulated in Eq. (5.6) is difficult to solve because it involves the normalization of W i.e., $\|W\|$ that includes square root. Quadratic optimization problem is designed to solve this problem in which $\|W\|$ is replaced by $\frac{1}{2}\|W\|^2$ without changing the solution. The modified optimization problem is:

$$\begin{aligned} &\arg\min_{(W,d)} \frac{1}{2}\|W\|^2 \\ &\textit{subject to} \quad Y_i(W \bullet X_i - d) \geq 1 \end{aligned} \tag{5.10}$$

The constrained problem in Eq. (5.7) can be expressed as follows by introducing Lagrange multipliers β :

$$\arg\min_{W,d} \max_{\beta \geq 0} \left\{ \frac{1}{2}\|W\|^2 - \sum_{i=1}^{z} \beta_i [Y_i(W \bullet X_i - d) - 1] \right\} \tag{5.11}$$

This optimization problem is solved using standard quadratic programming methods and programs. The solution to this problem can be expressed as a linear combination of training vectors.

$$W = \sum_{i=1}^{z} \beta_i Y_i X_i \tag{5.12}$$

The X_i corresponding to the β_i which are non zero, lies on the margin and are known as support vectors. These support vectors satisfy the following equation:

$$Y_i(W \bullet X_i - d) = 1 \tag{5.13}$$

This implies that:

$$d = W \bullet X_i - Y_i \tag{5.14}$$

This allows to calculate the offset d . This offset d depends on the X_i and Y_i .

5.1.2. Dual form

The dual problem is computationally easier to solve. The dual problem shows that the classification and maximum margin hyperplane depends only on the support vectors which are the subset of training data set. According to the dual problem the optimization problem is reduced as follows:

Maximize

$$\tilde{L}(\beta) = \sum_{i=1}^{z} \beta_i - \frac{1}{2} \sum_{i,j} \beta_i \beta_j Y_i Y_j X_i^T X_j = \sum_{i=1}^{z} \beta_i - \frac{1}{2} \beta_i \beta_j Y_i Y_j kr(X_i, X_j) \tag{5.15}$$

Subject to:

$$\beta_i \geq 0 \quad for\ all\ i = 1\ to\ z \tag{5.16}$$

and

$$\sum_{i=1}^{z} \beta_i Y_i = 0 \tag{5.17}$$

Where in Eq. (5.14) constraint from the minimization problem in d is included and the kernel in optimization problem is defined as:

$$kr(X_i X_j) = X_i \bullet X_j \tag{5.18}$$

The classification method chosen is support vector machine because the efficiency of SVM is superior from many other classifiers such as artificial neural network and Bayesian classifier.

CHAPTER 6

RESULTS AND DISCUSSION

The model of present work is described briefly using block diagram shown in figure 6.1.

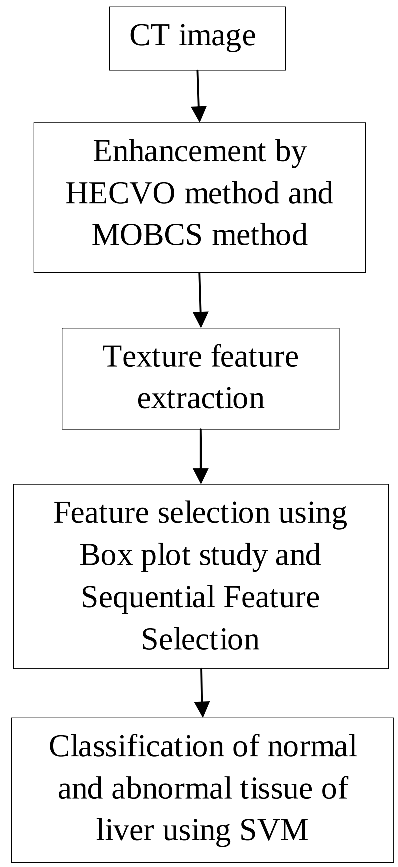

Figure 6.1 Block diagram of the present work

6.1 RESULTS OF ENHANCEMENT OF CT IMAGES

There are two enhancement methodologies proposed in the present work, they are modified object based contrast stretching (MOBCS) and histogram equalization with constrained variable offset (HECVO). Both of the methods are designed using MATLAB version 7.10.0 on a PC with Intel i5 processor. There are total 197 liver CT images out of which 20 images contains hepatocellular carcinoma (HCC) lesion, 82 images contains metastasis disease and remaining 95 images are the normal liver CT images. All the CT images are obtained from Max Saket hospital, Delhi. Both enhancement methods are applied on the 197 images and results are obtained. Quantitative performance analysis has been done to verify the enhancement results objectively.

6.1.1. Enhancement results of HECVO method

HECVO method is a global enhancement method which preserves the mean brightness of the enhanced image. This method basically overcomes the drawbacks of histogram equalization method such as over enhancement and saturation artifacts. The enhanced images by HECVO method show good visual details. The enhanced results compared with original images are shown in figure 6.2. The disease is marked with white circular marker in both original and enhanced images. Images A, B, C, D and E are original images and F, G, H, I and J are corresponding enhanced image results. Images A, B, C, F, G and H contains HCC liver lesion and the images D, E, I and J contains metastasis disease. The figure 6.2 shows that the visual quality of enhanced images is better than the original images. The details of information are clearer in the enhanced images than in original images.

6.1.2. Enhancement results of MOBCS method

MOBCS method enhances the textural portion of the CT image. It is local enhancement methodology which improves the local details of the image. All the parameters of the algorithm are tuned to obtain the best results of enhancement for CT images. First gradient threshold G_t is adjusted to obtain the gradient threshold magnitude map. The value of gradient threshold is adjusted to 0.15 times of the estimated standard deviation of noise σ_{noise} of the image. Then stopping condition δ_{sc} for region merging is tuned and at 5 times of standard deviation of noise best results are obtained. Then constraint variable λ which controls the contrast adjustment in greedy iterative stretching is tuned. The optimal value obtained for λ is 0.8. Finally the mean percentage variable α is varied to obtain the enhanced results. α is tuned and optimal value obtained is 30% of the mean of the corresponding image. All the parameters with their corresponding values obtained for the enhancement method MOBCS is shown in table 6.1. The image results obtained after all the parameter settings are the optimal results which improves the contrast and textural details with less distortion in the image while preserving the global outlook of the image.

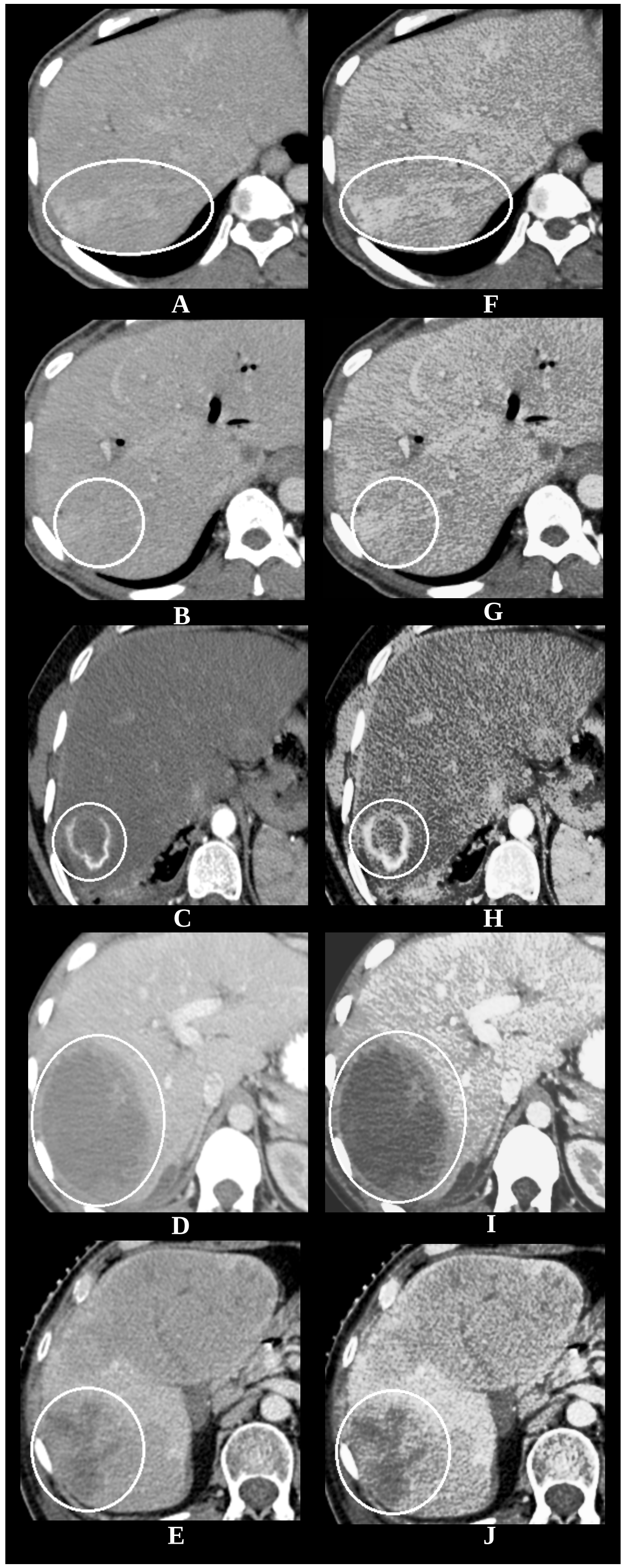

Figure 6.2 Comparisons of original CT images with enhanced images by HECVO method.

Table 6.1 Parameters of MOBCS method and their value tuned for the method

Parameter	Parameter value
G_t	$0.15\times\sigma_{noise}$
δ_{sc}	$5\times\sigma_{noise}$
λ	0.8
α	30%

The enhanced CT images by MOBCS method is shown in figure 6.3. In figure 6.3, images A, B, C, D and E are the original images and images F, G, H, I and J are the corresponding enhanced images by MOBCS method. The HCC and metastasis lesion is marked by white circular marker. The image results show that the enhanced images contain good visual quality and there is improvement in texture portion of the images.

6.1.3. Quantitative performance measures

Quantitative performance measures are calculated for objective evaluation of the enhancement methods. Five performance measures are chosen based on human visual system for quantitative analysis. These performance measures are calculated for all the images of CT liver images for both enhancement methods. Following quantitative performance measures are calculated for the objective evaluation:

1. Universal Image Quality Index (UQ): this is the measure of the distortion produced by the enhancement in the image [38, 39]. The mathematical formulation is shown as follows:

$$UQ = \frac{\sigma_{IE}}{\sigma_I \sigma_E} \cdot \frac{2\bar{E}\bar{I}}{(\bar{E})^2 + (\bar{I})^2} \cdot \frac{2\sigma_I \sigma_E}{\sigma^2{}_I + \sigma^2{}_E}, \quad -1 < UQ < 1 \tag{6.1}$$

Where $\bar{E}$ and $\bar{I}$ are the mean of the enhanced and original image respectively.

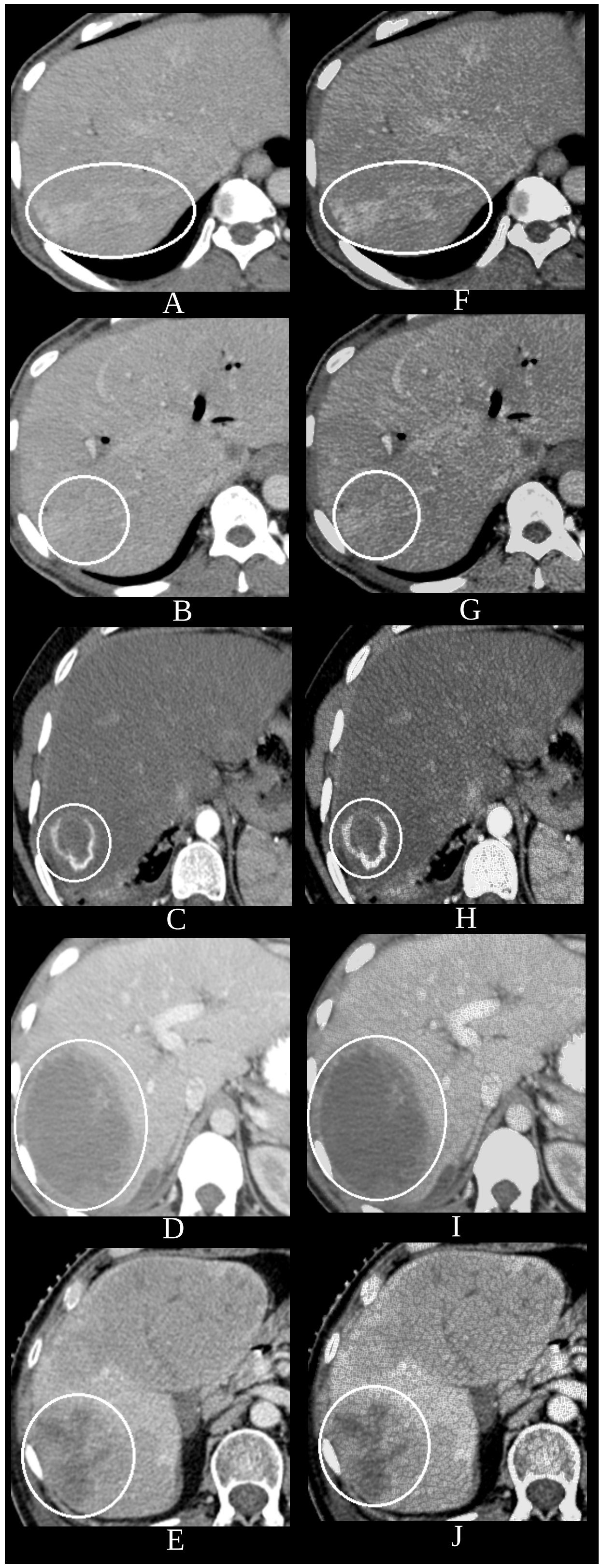

Figure 6.3 Comparisons of original CT images with enhanced images by MOBCS method.

2. Feature Similarity Index (FSIM): this is the measure of local image quality based on the features such as phase congruency and gradient magnitude map of the image [41]. The mathematical formulation of FSIM is as follows:

$$FSIM = \frac{\sum_{x,y\in\Omega} C_L(x,y)\cdot Ph_m(x,y)}{\sum_{x,y\in\Omega} Ph_m(x,y)} \tag{6.2}$$

where Ω shows spatial domain of the image, $Ph_m(x,y)$ is maximum of phase congruency between original and enhanced images and C_L is given as:

$$C_L(x,y) = \left[C_{Ph}(x,y)\right]^i \cdot \left[C_{Gd}(x,y)\right]^j \tag{6.3}$$

where C_{ph} and C_{gd} are the similarity measure of the phase and gradient between original and enhanced images respectively.

3. Correlation Coefficient (CC): this is the measure of amount of linear correlation between the original and enhanced images [39]. The mathematical formulation is shown as follows:

$$CC = \frac{\sum_{x=1}^{M}\sum_{y=1}^{N} E(x,y)I(x,y)}{\sqrt{\sum_{x=1}^{M}\sum_{y=1}^{N}(I(x,y))^2}\sqrt{\sum_{x=1}^{M}\sum_{y=1}^{N}(E(x,y))^2}} \tag{6.4}$$

Where E and I are the enhanced and original images with size M×N respectively.

4. Pratt's Figure of Merit (FOM): this is the measure of preservation of edges after enhancement operation [39]. The mathematical formulation of FOM is shown as follows:

$$FOM = \frac{1}{\max(Ed, Ed_{ideal})}\sum_{i=1}^{Ed}\frac{1}{1+g_i^{\,2}\tau} \tag{6.5}$$

Where Ed is detected edges, Ed_{ideal} is ideal edges, g is Euclidean distance between the detected pixel and its neighborhood pixels and τ is a constant term generally set to 1/9.

5. Mean Structural Similarity Index (MSSIM): this is the measure of structural similarity between original images and enhanced images [40]. The mathematical formulation of MSSIM is shown as follows:

$$MSSIM(I,E) = \frac{1}{O}\sum_{i=1}^{O} SSIM(I_i, E_i) \tag{6.6}$$

where SSIM is structural similarity measure between the original images and enhanced images at i^{th} local window and O is the total number of windows.

6.1.4. Comparison of results of HECVO and MOBCS method

HECVO method is a global enhancement method and MOBCS method is local and textural details enhancement method. Both methods enhance the CT images with good visual quality. The visual quality of enhanced images is verified by the objective evaluation by quantitative performance measures. The quantitative performance measures are calculated on the total database for enhancement method HECVO and MOBCS method. Then mean and variance of all performance measures is calculated to reduce sample bias. The mean and variance of the performance measures for both methods are compared in table 6.2.

The universal image quality index (UQ) shows the distortion measure between the original image and enhanced image. The range of UQ is -1 to 1. Higher values of UQ show less distortion in the enhanced image. The mean value of UQ for results of MOBCS method is 0.9421 and the minimum value is 0.9330 and maximum value is 0.9575. The mean value of UQ for results of HECVO method is 0.9144, the minimum and maximum values are 0.8130 and 0.9693 respectively. This result shows that, MOBCS enhancement method shows less distortion in comparison to HECVO method.

Feature similarity index (FSIM) measures the similarity in the features of original image and enhanced image and local quality of the image. Higher values of FSIM show better image local quality and more similarity to the original image. The mean value of FSIM for MOBCS method is 0.9378, minimum and maximum values are 0.9196 and 0.9453 respectively. The mean value of FSIM for HECVO method is 0.7942, minimum and maximum values are 0.6776 and 0.8520 respectively. This result shows that, enhanced image result obtained by MOBCS is more similar to original image then HECVO method.

Table 6.2 Comparison of performance measures

Performance measures	HECVO	MOBCS
UQ	$0.9144 \pm 1.4550 \times 10^{-03}$	$0.9421 \pm 3.8845 \times 10^{-05}$
FSIM	$0.7942 \pm 2.1070 \times 10^{-03}$	$0.9378 \pm 2.9496 \times 10^{-05}$
CC	$0.9872 \pm 3.1298 \times 10^{-05}$	$0.9929 \pm 5.5659 \times 10^{-06}$
FOM	$0.5798 \pm 1.7507 \times 10^{-02}$	$0.6601 \pm 1.2709 \times 10^{-02}$
MSSIM	$0.5091 \pm 2.1730 \times 10^{-02}$	$0.8378 \pm 9.0932 \times 10^{-04}$

Correlation coefficient (CC) shows the linear correlation between original and enhanced images. The dynamic range of CC is [-1,1]. The value -1 shows negative correlation and +1 shows highest correlation between two images. The mean value of CC for MOBCS method is 0.9929, minimum and maximum values are 0.9870 and 0.9950 respectively. The mean value of CC for HECVO method is 0.9872, minimum and maximum values are 0.9702 and 0.9927 respectively. The CC value of MOBCS method is greater than HECVO method, this show that enhanced results obtained by MOBCS method have greater correlation with original image in comparison to HECVO method.

Pratt’s figure of merit (FOM) shows the edge preservation in the enhanced images. The dynamic range of FOM is [0, 1]. Higher values show good preservation of edges in the images. The mean value of FOM for MOBCS method is 0.6601, minimum and maximum values obtained for the data set are 0.4915 and 0.8672 respectively. The mean value of FOM for HECVO method is 0.5798, minimum and maximum values of FOM are 0.3627 and 0.8183 respectively. This result shows that MOBCS method performs better from HECVO method for FOM.

Mean structural similarity index (MSSIM) shows the structural similarity between two images. The value of MSSIM closer to 1 shows high similarity between two images. The mean value of MSSIM for MOBCS method is 0.8378, the minimum and maximum values calculated are 0.7648 and 0.8759 respectively. The mean value of MSSIM for HECVO method is 0.5091, the minimum and maximum calculated value are 0.1188 and 0.6844 respectively. This shows that structural similarity of the enhanced results obtained by MOBCS method is higher than the

HECVO method. MOBCS method outperforms the HECVO method for all the five performance measures. The comparison of the distribution of results of the performance measures calculated for both enhancement methods is shown in figure 6.4 through box plots. Images A, B, C, D and E in figure 6.4 shows the box plot of universal image quality index, feature similarity index, correlation coefficient, Pratt's figure of merit and mean structural similarity index respectively.

In conclusion, both enhancement methods MOBCS and HECVO methods show better visual details of information than original image. According to the objective performance evaluation MOBCS method shows better results in comparison to the HECVO method. The result of performance evaluation shows that enhanced images obtained after applying MOBCS method have better enhancement and less distortion in the image, enhanced images are more similar to original image which mean information of original image is preserved in the enhanced image.

6.2 RESULTS OF TEXTURE FEATURE EXTRACTION

MOBCS method enhances the texture part of the CT images; this is visible in the enhancement image results. So to verify the enhancement of textural details through MOBCS method texture feature extraction and classification is done. Classification of normal and cancerous tissue of liver is done in present work. Then the accuracy of classification of images obtained by MOBCS method and original images is compared. All the seven methods of texture features extraction explained in chapter -4, are calculated on the original image Org, image enhanced by HECVO method IE1 and image enhanced by MOBCS method IE2. There are total 300 CT images of size 22x27 of liver tissue, from which 150 are normal liver tissue images and remaining 150 are cancerous liver tissue images. The texture features are extracted on total 300 liver CT images for three set of images i.e., Org, IE1and IE2. The total features calculated are shown in table 6.1. For further using these features in classification of normal and abnormal tissue, feature selection is required to reduce the redundancy and increase the efficiency of classification. First feature selection is done on the basis of Box plot study. Box plots are drawn for visualizing the difference in inter classes of the texture features calculated. Those features are selected whose interclass difference is high. According to the Box plot study the features selected for the further classification are 32 features and they are shown in table 6.4.

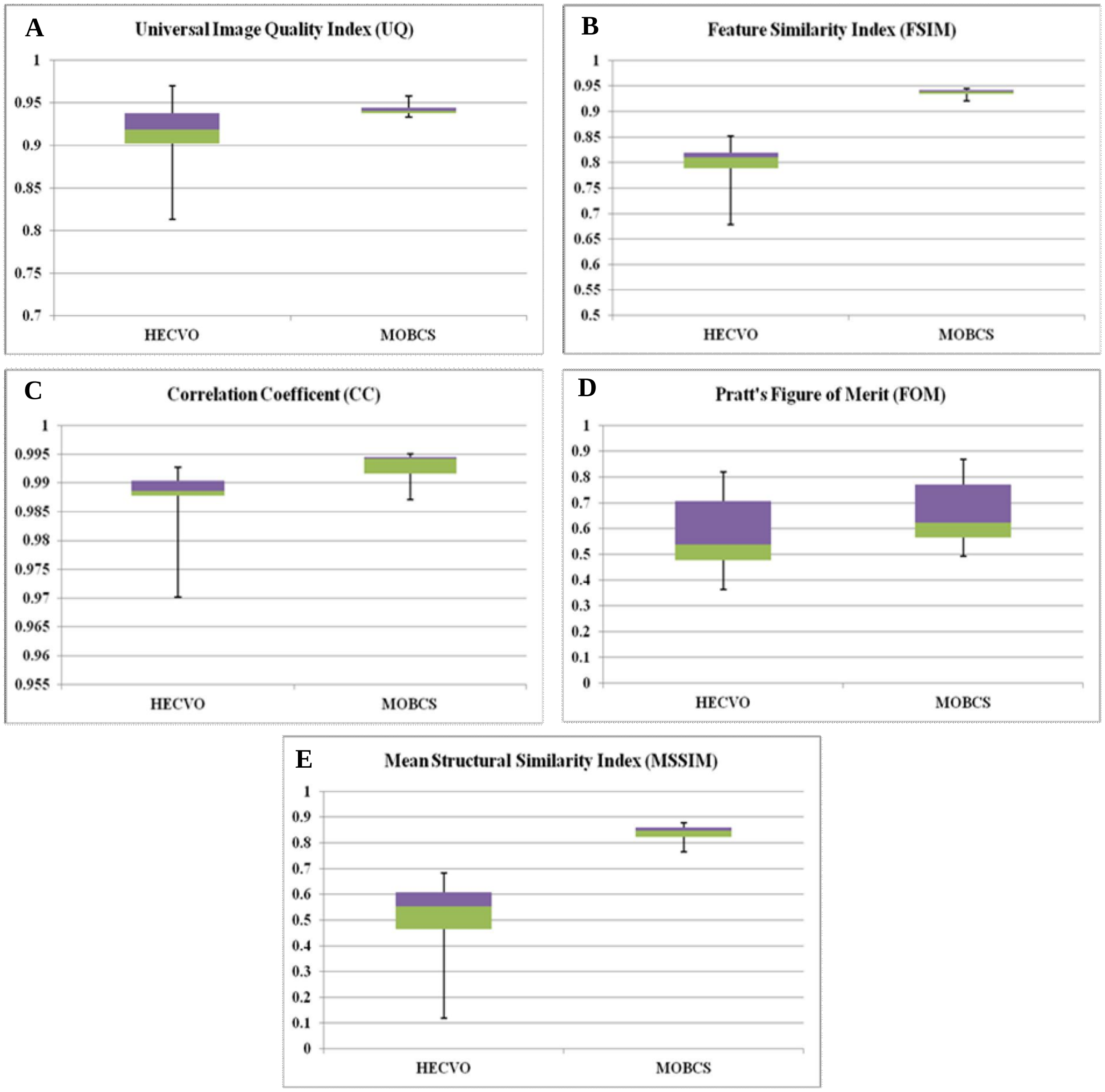

Figure 6.4 Comparison box plots of performance measures calculated for HECVO and MOBCS method

The box plot for all the features are shown in Appendix. On the basis of Box plot study the images enhanced by HECVO method are excluded from the classification and feature selection study because HECVO method enhances the image globally, texture details are not much improved . This shows that the image results obtained by HECVO method show good visual quality but improvement in texture are not efficient.

Table 6.3 total features extracted

Sr. No.	Features	No. of features
1	GLCM	13×4=52
2	GLRLM	11
3	GTDM	7
4	Hu moments	7
5	Zernike moments	3
6	Gabor features	40
7	FOS	6
8	Statistical features Matrix	4
	Total features	130

Table 6.4 selected features based on box plot study

Sr. No.	Selected features
1	Sum entropy
2	Angular second moment
3	Correlation
4	Inverse difference moment
5	Sum average
6	Sum variance
7	Entropy
8	Difference variance
9	Difference entropy
10	Information measure1 of correlation
11	Information measure2 of correlation
12	SRE
13	GLN
14	RP
15	LGRE
16	HGRE
17	SRLGE
18	SRHGE
19	Busyness
20	Complexity
21	Contrast
22	Strength
23	Hu moment 1
24	Hu moment 2
25	zernike moment (0,0)
26	zernike moment (2,0)
27	Mean
28	Energy

29	Variance
30	Gabor features
31	Periodicity
32	Roughness

After selecting features using Box plot study, seqential feature selection criterion is used for further selection of the features to reduce the over fitting. The features selected on the basis of sequential feature selection are 8. The features selected after sequential feature selction are shown in table 6.5.

Table 6.5 Features selected on the basis of sequential feature selection method

Sr. No.	Selected Features
1	Angular second Moment
2	Difference entropy
3	Busyness
4	Strength
5	Hu moment 2
6	Energy
7	SRLGE
8	SRHGE

There are total 8 features selected on the basis of the sequential feature selection method. These are angular second moment, difference entropy, busyness, strength, Hu moment-2, energy, SRLGE and SRHGE. The inter class difference for angular second moment feature is sufficiently high, due which two classes can be classified easily without any misclassification. The value of angular second moment for normal liver tissue is higher than the abnormal tissue. The texture values of busyness, energy, Hu moment 2 and SRHGE are also greater for normal liver tissue and lesser for abnormal tissue. The value of difference entropy, strength and SRLGE for normal liver tissue is less than abnormal tissue. The features selected have difference in the values for normal and abnormal tissue. The inter class difference of texture features is increased for the enhanced images and it is higher than original images.the features selected assists in caracterization of the normal and abnormal liver tissue.

6.3 RESULTS OF CLASSIFICATION

In present work support vector machine is used for classification of the normal and abnormal tissue. There are total 300 liver image samples from which 150 are normal liver images and 150 are abnormal i.e, cancerous liver images. First enhancement methodology MOBCS is applied to all the images and then images is cropped in size 22x27 for texture analysis study. After texture feature extraction and feature selection, SVM classification is applied on both original and enhanced images by MOBCS method. svmtrain and svmclassify are the two function functions used for training and classification. The training data selected from the whole data set are 200 for each feature and remaining 100 data for each feature are selected for test data. Training is done by using function svmtrain. This function generates a SVM model, the main fields present in this model is explained as follows:

Support vectors: this is a matrix in which each row corresponds to the support vectors of the data points. This matrix is the sub set of the training data set.

Alpha: this is a vector containing weights for the support vectors. The positive values in this vector indicate the support vector belonging to class first and the negative value indicates the support vector belonging to class second.

Bias: it is the intercept of the hyperplane that separates the two classes.

Kernel function: it is a function handle that maps the training data into kernel space.

Scale data: this is a structure that contains normalization factors and it has two fields

- Shift: it is row vector in which each value is the negative of the mean across an observation in training the training data.
- Scale factor: it is a row vector in which each value is 1 divided by the standard deviation of an observation in training the training data.

The SVM model obtained for classification of original images for selected features is shown as follows:

Support vectors: matrix of size 123x8

Alpha: matrix of size 123x1

Bias: -0.2720

Kernel function: rbf_kernel

Scale data: shift- matrix of size 1x8 and scale factor- matrix of size 1x8

The SVM model obtained for classification of enhanced images for selected features is as follows:

Support vectors: matrix of size 147x8

Alpha: matrix of size 147x1

Bias: -0.3384

Kernel function: rbf_kernel

Scale data: shift- matrix of size 1x8 and scale factor- matrix of size 1x8

By using these SVM models classification of normal and cancerous tissue is done for both original image data and enhanced image data. After classification confusion matrix is obtained. The confusion matrix obtained from the classification of original image data is shown in table 6.6. Total test data are 100 from which 50 data are normal tissue data and rest 50 data are abnormal tissue. In classification of original image data, all 50 data of abnormal tissue are predicted correctly and 45 data of normal tissue is predicted correctly and remaining 5 data is predicted as abnormal tissue.

Accuracy, sensitivity and specificity of classification of original image data is shown in Eq.(6.7), Eq.(6.8), and Eq.(6.9) respectively.

$$acc_o = \frac{50+45}{100} \times 100 = 95\% \tag{6.7}$$

$$sen_o = \frac{50}{50+0} \times 100 = 100\% \tag{6.8}$$

$$spe_o = \frac{45}{45+5} \times 100 = 90\% \tag{6.9}$$

Table 6.6 Confusion matrix of classification of original image data

		Predicted class	
		Abnormal tissue	Normal tissue
Actual class	Abnormal tissue	50	0
	Normal tissue	5	45

The confusion matrix obtained from the classification of enhanced image data is shown in table 6.7. In classification of enhanced image data, 49 data of abnormal tissue are predicted correctly and one data is abnormal and predicted as normal and all 50 data of normal tissue is predicted correctly.

Table 6.7 Confusion matrix of classification of enhanced image data

		Predicted class	
		Abnormal tissue	Normal tissue
Actual class	Abnormal tissue	49	1
	Normal tissue	0	50

Accuracy, sensitivity and specificity of classification of enhanced image data is shown in Eq.(6.10), Eq.(6.11), and Eq.(6.12) respectively.

$$acc_e = \frac{49+50}{100} \times 100 = 99\% \tag{6.10}$$

$$sen_e = \frac{49}{49+1} \times 100 = 98\% \tag{6.11}$$

$$spe_e = \frac{50}{50+0} \times 100 = 100\% \tag{6.12}$$

6.4 DISCUSSION

The classification of the normal and abnormal liver tissue of the CT images is done using texture features calculated on the images. the accuracy of classification results of original image data is 95%, this means that out of 100 liver CT image test data 95 test data is correctly detected. The accuracy of classification of enhanced image data is 99%, this means out of 100 test data 99 cases are correctly detected. This result shows that enhancement method MOBCS improves the textural details of the CT images and the enhancement method is helpul in better disease detection. The enhancement by MOBCS method made detection of disease is easier in both ways, by visual inspection and also by classification of the images. the classification accuracy proves that MOBCS method is an effective enhancement method for detection of tumor in the CT images.

CHAPTER 7

CONCLUSION

Enhancement of CT images and classification of normal and abnormal tissue in enhanced images is compared with the original image in the present work. The enhancement of CT images is done by proposing two methods of enhancement. The histogram equalization with constrained variable offset (HECVO) method enhances the global contrast of the CT scan images. This method improves the visual details and can be used for visual inspection of disease using CT images. The modified object based contrast stretching (MOBCS) method is used to enhance the local details of the CT images by enhancing the texture of the CT images. To verify the texture enhancement done using MOBCS method texture feature extraction and classification of normal and abnormal tissue is done and compared the classification results of enhanced images with the original images. The results of classification using support vector machine show that the enhanced images improves the texture such that the normal and abnormal tissue is classified with 99% accuracy whereas original images shows the accuracy of 95%. This shows that MOBCS method is an effective enhancement method for CT images for both visual inspection and computer aided diagnosis and HECVO method is effective enhancement which assists in diagnosis using visual inspection by radiologists.

REFERENCES

[1] Available at http://www.sprawls.org/resources/CTIMG/module.htm#1

[2] Yu, Yang, and Hong Zhao. "A texture-based Morphologic Enhancement Filter in Two-dimensional Thoracic CT scans." *Networking, Sensing and Control, 2006. ICNSC'06. Proceedings of the 2006 IEEE International Conference on*. IEEE, 2006.

[3] Mir, A. H., et al. "Combining texture parameters with fuzzy logic based image enhancement for identification of diseases in ct images." *e-Health Networking, Applications and Services, 2006. HEALTHCOM 2006. 8th International Conference on*. IEEE, 2006.

[4] Jafar, Iyad, and Hao Ying. "Image contrast enhancement by constrained variational histogram equalization." *Electro/Information Technology, 2007 IEEE International Conference on*. IEEE, 2007.

[5] Wu, Pei-Chen, Fan-Chieh Cheng, and Yu-Kumg Chen. "A weighting mean-separated sub-histogram equalization for contrast enhancement." *Biomedical Engineering and Computer Science (ICBECS), 2010 International Conference on*. IEEE, 2010.

[6] Xu, Beilei, et al. "Object-based multilevel contrast stretching method for image enhancement." *Consumer Electronics, IEEE Transactions on* 56.3 (2010): 1746-1754.

[7] Hsu, Wei-Tai, et al. "A computer aided for image processing of computed tomography in hepatocellular carcinoma." *Bioinformatics and Biomedicine Workshops (BIBMW), 2011 IEEE International Conference on*. IEEE, 2011.

[8] Sajjadi, Mehdi, et al. "A new filter bank algorithm for enhancement of early signs of ischemic stroke in brain CT images." *Signal and Image Processing Applications (ICSIPA), 2011 IEEE International Conference on*. IEEE, 2011.

[9] Sajjadi, Mehdi, Rassoul Amirfattahi, and Mohammad Reza Ahmadzadeh. "A New NSCT Based Contrast Enhancement Algorithm for Amplification of Early Signs of Ischemic Stroke in Brain CT Images." *Machine Vision and Image Processing (MVIP), 2011 7th Iranian*. IEEE, 2011.

[10] Rudzki, Marcin. "Automatic image contrast enhancement method for liver vasculature detection." *Mixed Design of Integrated Circuits and Systems (MIXDES), 2011 Proceedings of the 18th International Conference*. IEEE, 2011.

[11] Tan, Tiong-Lang, Kok-Swee Sim, and Aun-Kee Chong. "Contrast enhancement of ct brain images for detection of ischemic stroke." *Biomedical Engineering (ICoBE), 2012 International Conference on*. IEEE, 2012.

[12] Al-Ameen, Zohair, Ghazali Sulong, and Md Gapar Md Johar. "Enhancing the Contrast of CT Medical Images by Employing a Novel Image Size Dependent Normalization Technique." *International Journal of Bio-Science and Bio-Technology* 4.3 (2012): 63-68.

[13] An, Vu Thanh, and Nguyen Thanh Hai. "Enhancement of CT image using image fusion." *Advanced Technologies for Communications (ATC), 2013 International Conference on*. IEEE, 2013.

[14] Jalab, Hamid A., and Rabha W. Ibrahim. "Texture enhancement for medical images based on fractional differential masks." *Discrete Dynamics in Nature and Society* 2013 (2013).

[15] Celik, Turgay. "Spatial entropy-based global and local image contrast enhancement." *Image Processing, IEEE Transactions on* 23.12 (2014): 5298-5308.

[16] Agarwal, Tarun K., Mayank Tiwari, and Subir Singh Lamba. "Modified histogram based contrast enhancement using homomorphic filtering for medical images." *Advance Computing Conference (IACC), 2014 IEEE International*. IEEE, 2014.

[17] Malik, Showkat Hassan, Tariq Ahmad Lone, and S. M. K. Quadri. "Contrast Enhancement and Smoothing of CT Images for Diagnosis." *2015 2nd International Conference on Computing for Sustainable Global Development (INDIACom),* IEEE,2015.

[18] Al-Ameen, Zohair, and Ghazali Sulong. "A new algorithm for improving the low contrast of computed tomography images using tuned brightness controlled single-scale Retinex." *Scanning* 37.2 (2015): 116-125.

[19] Wang, Jing-jing, et al. "Medical image enhancement algorithm based on NSCT and the improved fuzzy contrast." *International Journal of Imaging Systems and Technology* 25.1 (2015): 7-14.

[20] Bilello, Michel, et al. "Automatic detection and classification of hypodense hepatic lesions on contrast-enhanced venous-phase CT." *Medical physics* 31.9 (2004): 2584-2593.

[21] Arivazhagan, S., L. Ganesan, and TG Subash Kumar. "Texture classification using ridgelet transform." *Pattern Recognition Letters* 27.16 (2006): 1875-1883.

[22] Zhang, Wei-Li, and Xi-Zhao Wang. "Feature extraction and classification for human brain CT images." *Machine Learning and Cybernetics, 2007 International Conference on*. Vol. 2. IEEE, 2007.

[23] Bharathi, V. Subbiah, and L. Ganesan. "Orthogonal moments based texture analysis of CT liver images." *Pattern Recognition Letters* 29.13 (2008): 1868-1872.

[24] Masotti, Matteo, and Renato Campanini. "Texture classification using invariant ranklet features." *Pattern Recognition Letters* 29.14 (2008): 1980-1986.

[25] Lee, Youngjoo, et al. "Performance testing of several classifiers for differentiating obstructive lung diseases based on texture analysis at high-resolution computerized tomography (HRCT)." *Computer methods and programs in biomedicine* 93.2 (2009): 206-215.

[26] Basu, Satrajit, et al. "Developing a classifier model for lung tumors in CT-scan images." *Systems, Man, and Cybernetics (SMC), 2011 IEEE International Conference on*. IEEE, 2011.

[27] Sun, Tao, et al. "Comparative evaluation of support vector machines for computer aided diagnosis of lung cancer in CT based on a multi-dimensional data set." *Computer methods and programs in biomedicine* 111.2 (2013): 519-524.

[28] Devan, Lakshmi, Roy Santosham, and Ranganathan Hariharan. "Automated texture-based characterization of fibrosis and carcinoma using low-dose lung CT images." *International Journal of Imaging Systems and Technology* 24.1 (2014): 39-44.

[29] Kayaaltı, Ömer, et al. "Liver fibrosis staging using CT image texture analysis and soft computing." *Applied Soft Computing* 25 (2014): 399-413.

[30] Khalilinezhad, Mahdieh, Silvana Dellepiane, and Gianni Vernazza. "Detecting HCC Tumor in Three Phasic CT Liver Images with Optimization of Neural Network." *International Journal of Medical, Health, Biomedical and Pharmaceutical Engineering* 9.3 (2015): 262-267.

[31] Mala, K., V. Sadasivam, and S. Alagappan. "Neural network based texture analysis of CT images for fatty and cirrhosis liver classification." *Applied Soft Computing* 32 (2015): 80-86.

[32] Sharma, Kanika, and Deepti Mittal. "Contrast Enhancement Technique for CT Images." *Journal of Biomedical Engineering and Medical Imaging* 2.1 (2015): 44.

APPENDIX

Box plots of features for feature selection using box plot study.

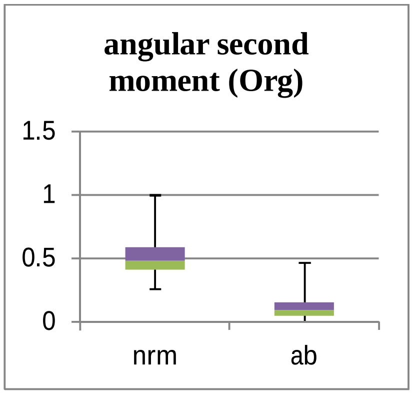

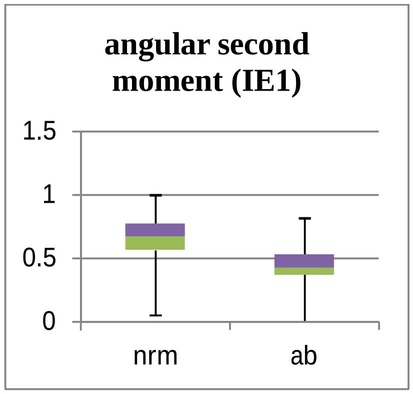

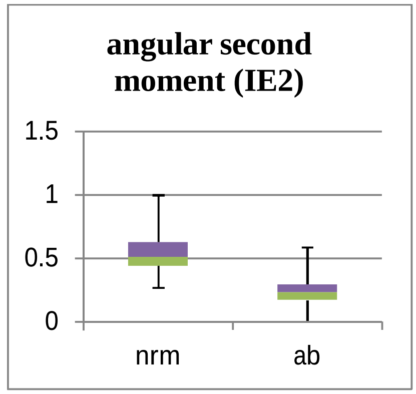

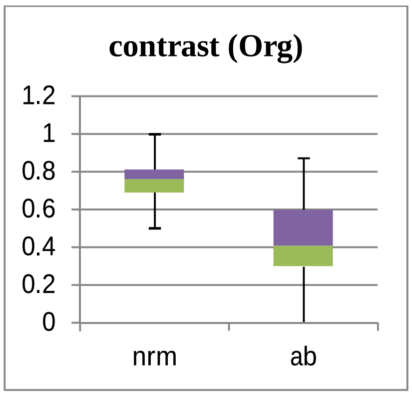

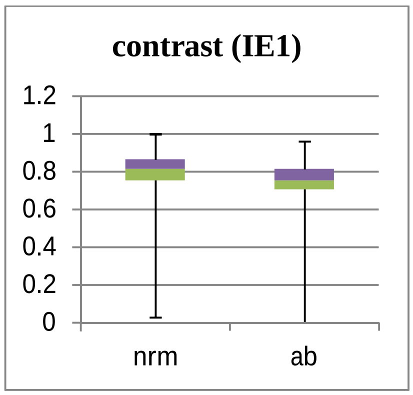

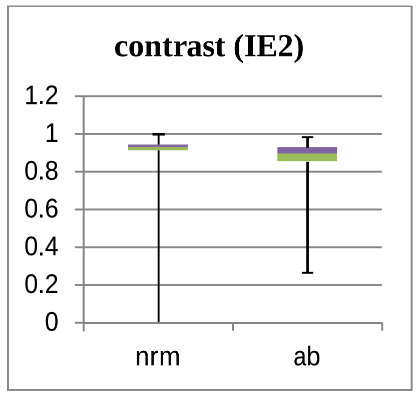

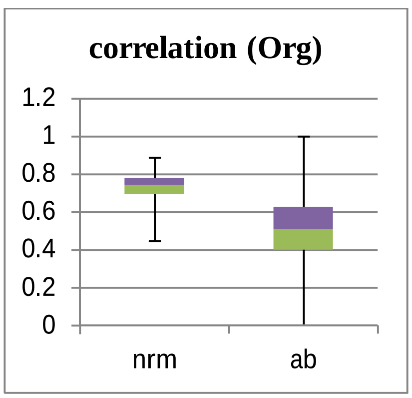

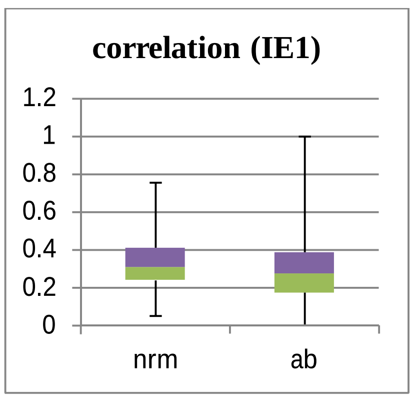

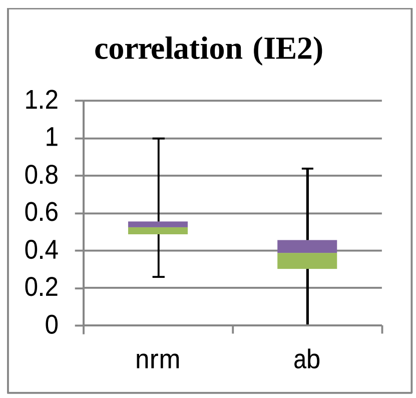

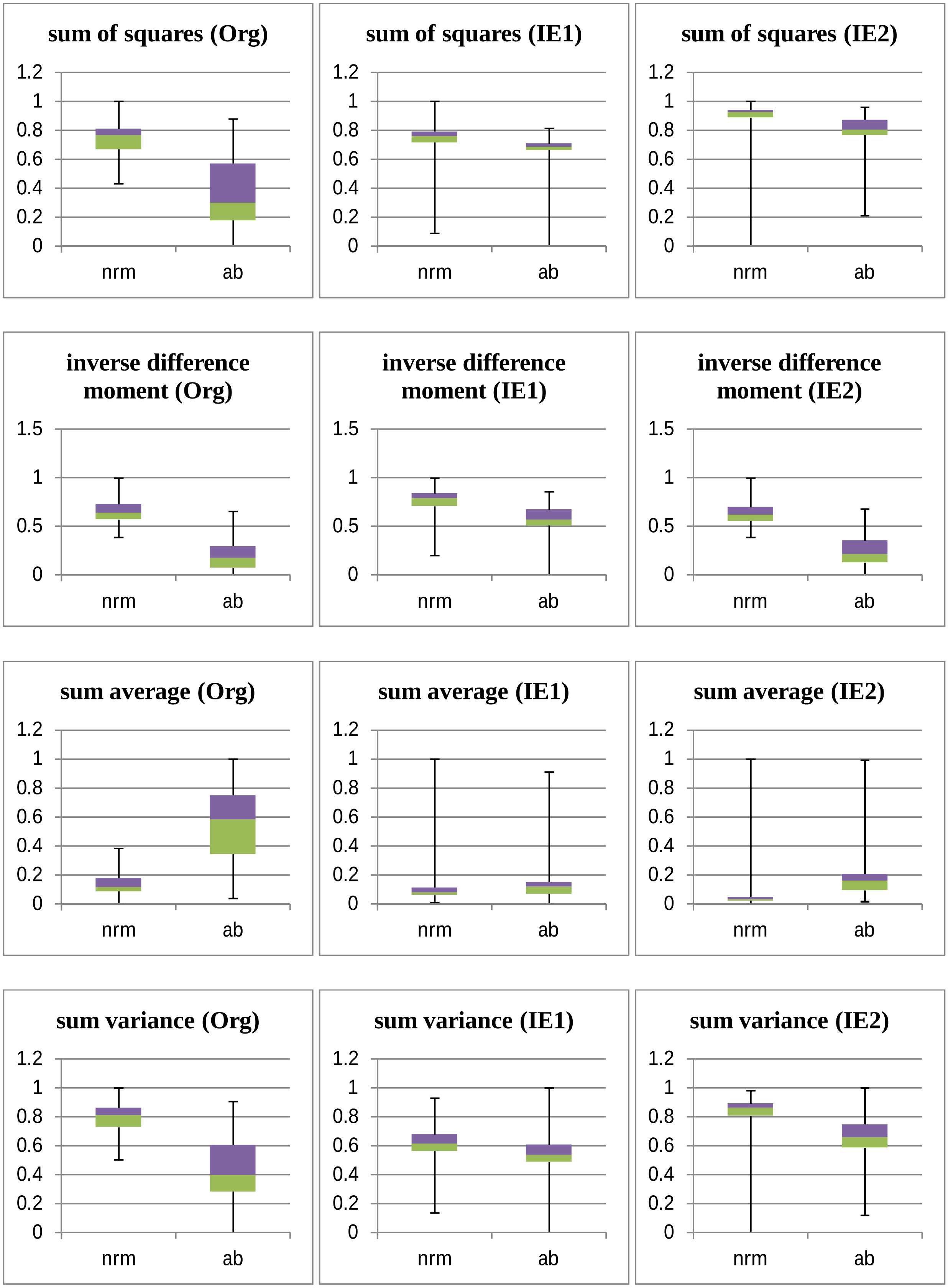
sum of squares (Org)
sum of squares (IE1)
sum of squares (IE2)
inverse difference moment (Org)
inverse difference moment (IE1)
inverse difference moment (IE2)
sum average (Org)
sum average (IE1)
sum average (IE2)
sum variance (Org)
sum variance (IE1)
sum variance (IE2)
0
0.2
0.4
0.5
0.6
0.8
1
1.2
1.5
nrm
ab

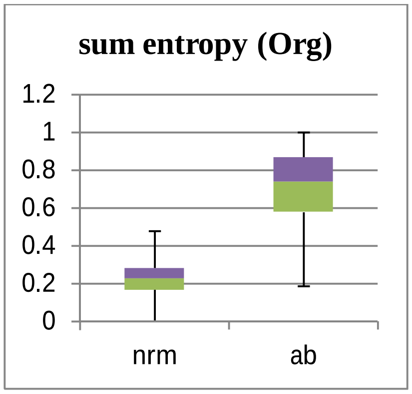
sum entropy (Org)
1.2
1
0.8
0.6
0.4
0.2
0
nrm
ab

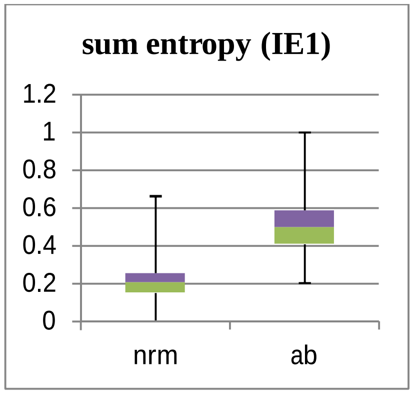
sum entropy (IE1)
1.2
1
0.8
0.6
0.4
0.2
0
nrm
ab

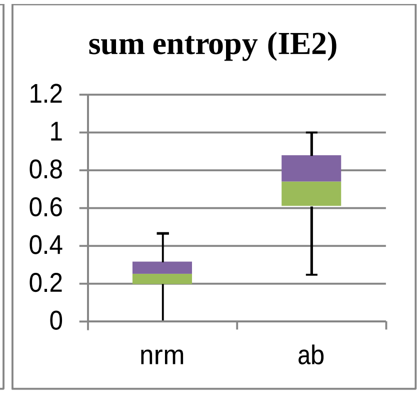
sum entropy (IE2)
1.2
1
0.8
0.6
0.4
0.2
0
nrm
ab

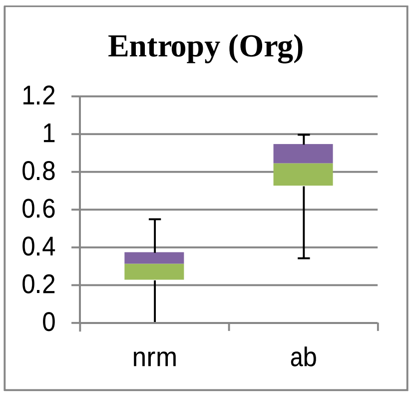
Entropy (Org)
1.2
1
0.8
0.6
0.4
0.2
0
nrm
ab

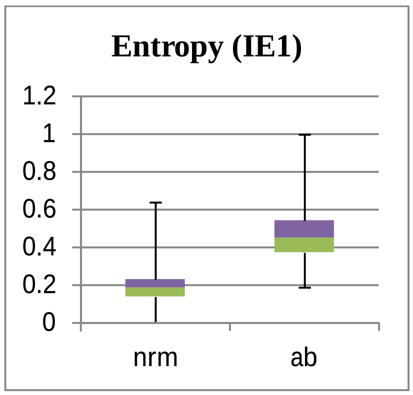
Entropy (IE1)
1.2
1
0.8
0.6
0.4
0.2
0
nrm
ab

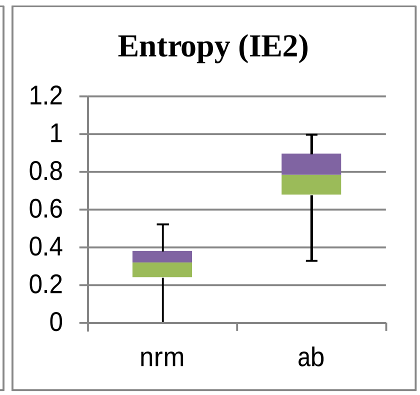
Entropy (IE2)
1.2
1
0.8
0.6
0.4
0.2
0
nrm
ab

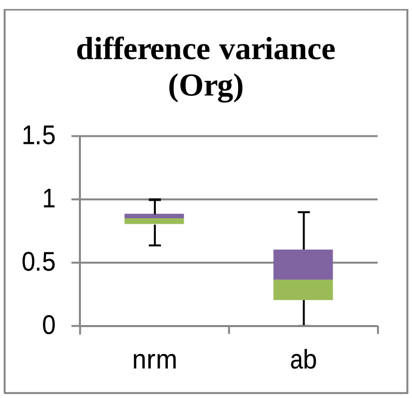
difference variance (Org)
1.5
1
0.5
0
nrm
ab

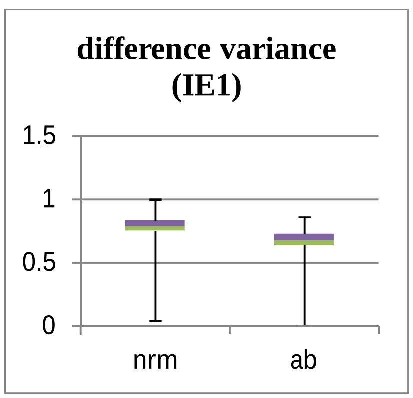
difference variance (IE1)
1.5
1
0.5
0
nrm
ab

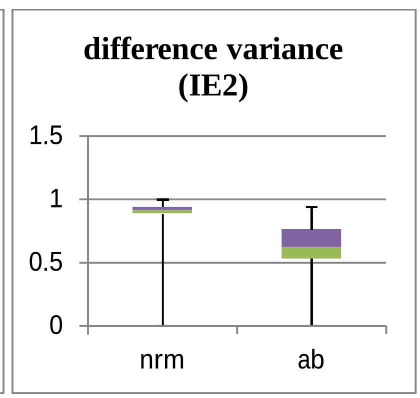
difference variance (IE2)
1.5
1
0.5
0
nrm
ab

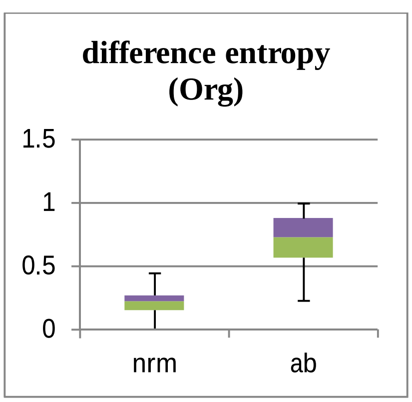
difference entropy (Org)
1.5
1
0.5
0
nrm
ab

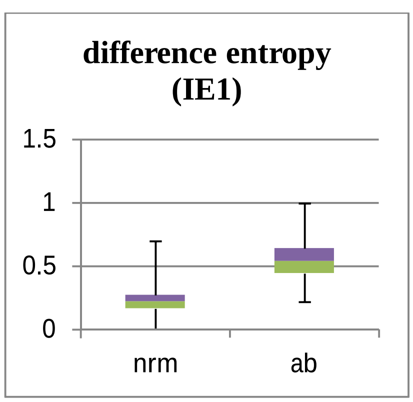
difference entropy (IE1)
1.5
1
0.5
0
nrm
ab

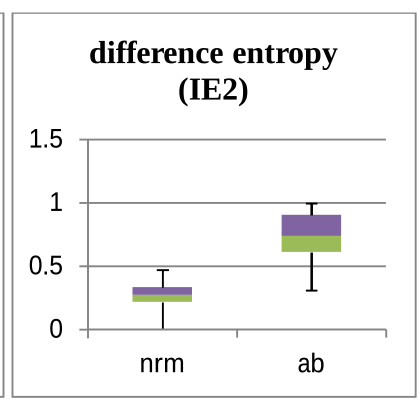
difference entropy (IE2)
1.5
1
0.5
0
nrm
ab

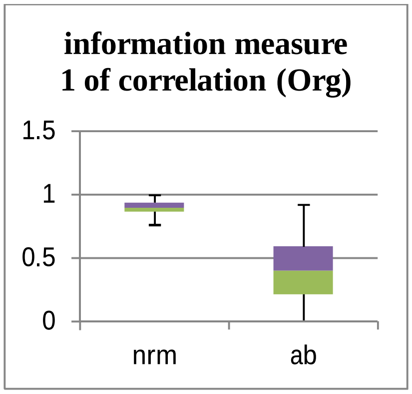
information measure
1 of correlation (Org)
1.5
1
0.5
0
nrm
ab

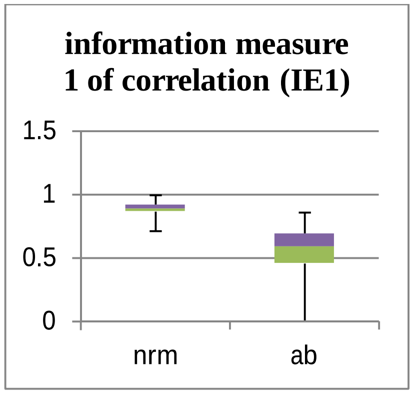
information measure
1 of correlation (IE1)
1.5
1
0.5
0
nrm
ab

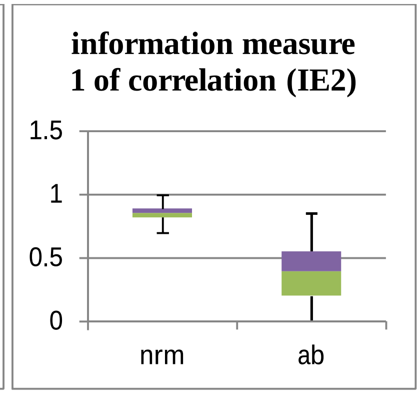
information measure
1 of correlation (IE2)
1.5
1
0.5
0
nrm
ab

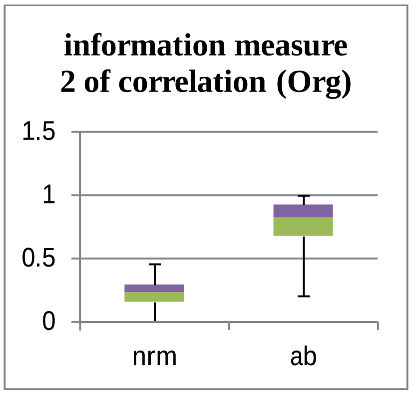
information measure
2 of correlation (Org)
1.5
1
0.5
0
nrm
ab

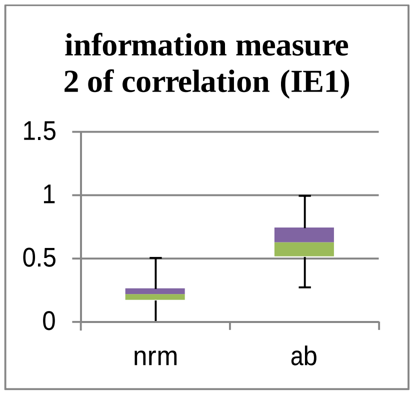
information measure
2 of correlation (IE1)
1.5
1
0.5
0
nrm
ab

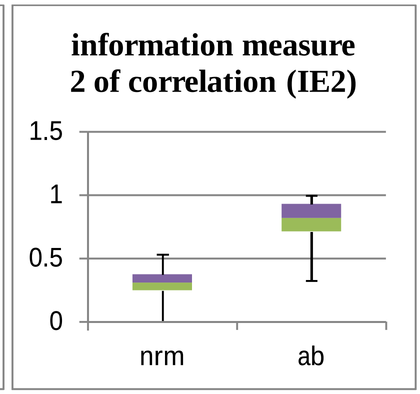
information measure
2 of correlation (IE2)
1.5
1
0.5
0
nrm
ab

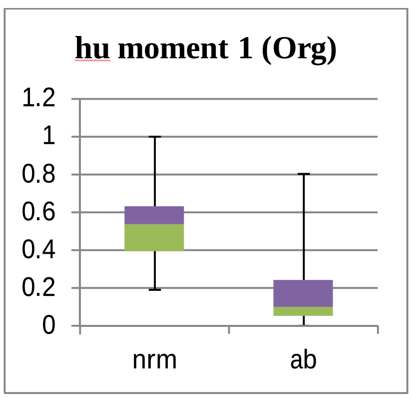
hu moment 1 (Org)
1.2
1
0.8
0.6
0.4
0.2
0
nrm
ab

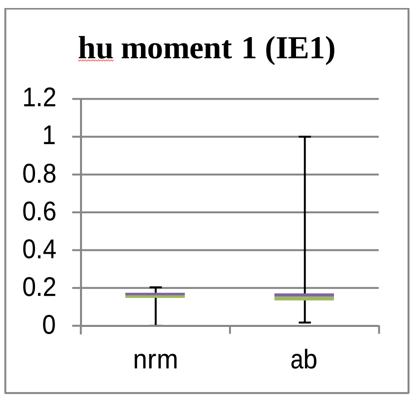
hu moment 1 (IE1)
1.2
1
0.8
0.6
0.4
0.2
0
nrm
ab

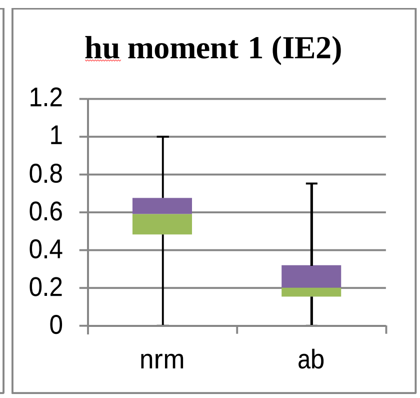
hu moment 1 (IE2)
1.2
1
0.8
0.6
0.4
0.2
0
nrm
ab

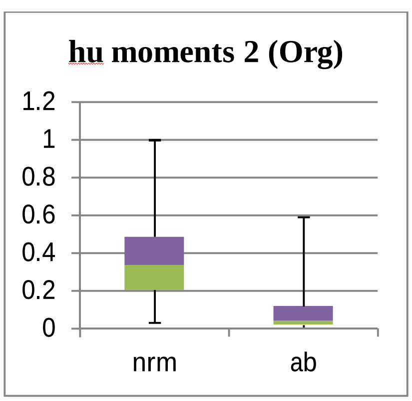
hu moments 2 (Org)
1.2
1
0.8
0.6
0.4
0.2
0
nrm
ab

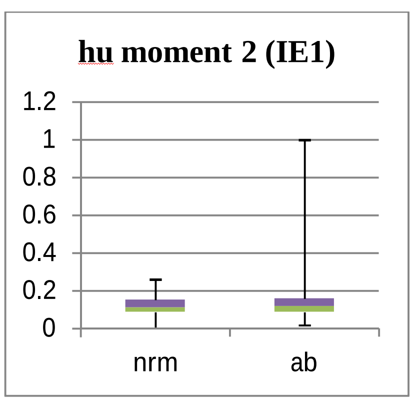
hu moment 2 (IE1)
1.2
1
0.8
0.6
0.4
0.2
0
nrm
ab

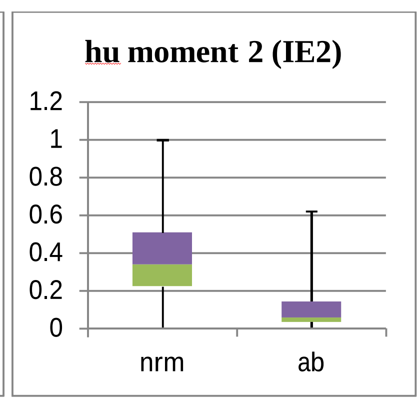
hu moment 2 (IE2)
1.2
1
0.8
0.6
0.4
0.2
0
nrm
ab

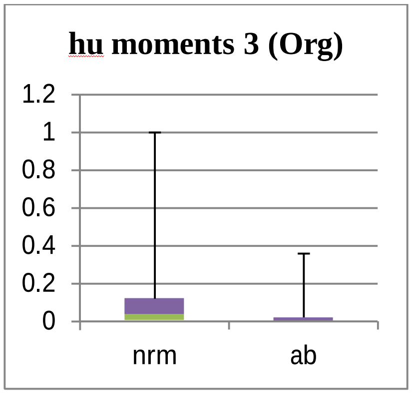
hu moments 3 (Org)
1.2 1 0.8 0.6 0.4 0.2 0
nrm ab

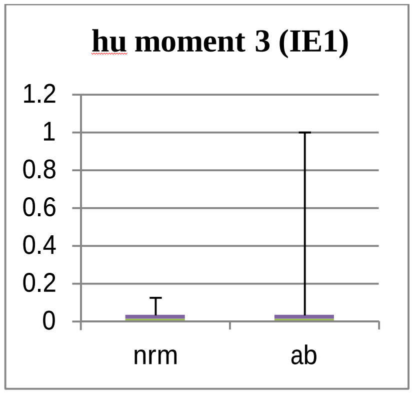
hu moment 3 (IE1)
1.2 1 0.8 0.6 0.4 0.2 0
nrm ab

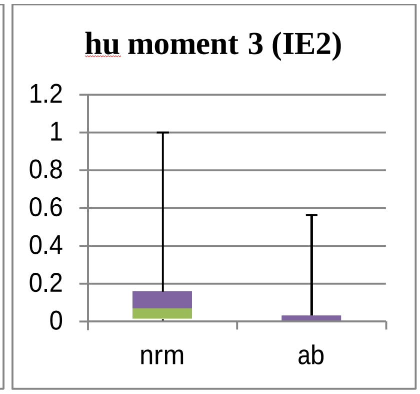
hu moment 3 (IE2)
1.2 1 0.8 0.6 0.4 0.2 0
nrm ab

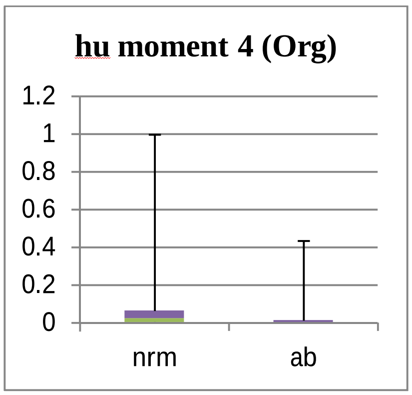
hu moment 4 (Org)
1.2 1 0.8 0.6 0.4 0.2 0
nrm ab

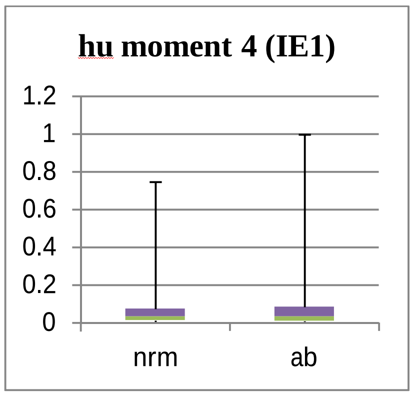
hu moment 4 (IE1)
1.2 1 0.8 0.6 0.4 0.2 0
nrm ab

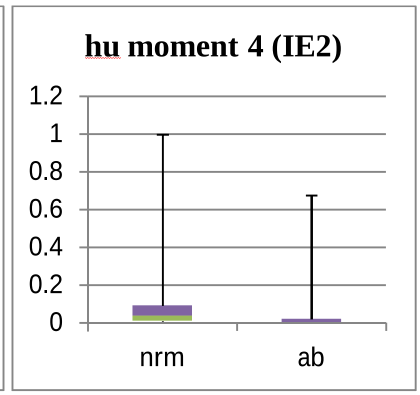
hu moment 4 (IE2)
1.2 1 0.8 0.6 0.4 0.2 0
nrm ab

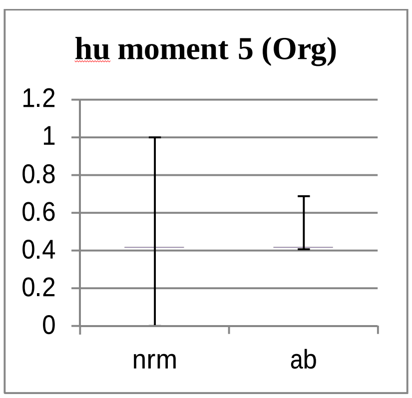
hu moment 5 (Org)
1.2 1 0.8 0.6 0.4 0.2 0
nrm ab

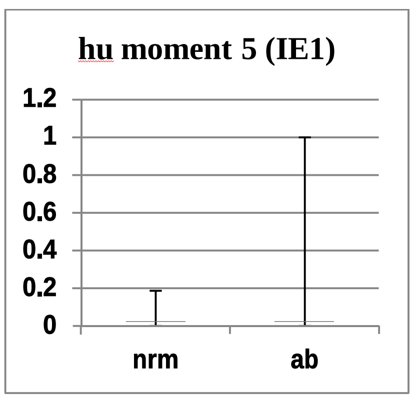
hu moment 5 (IE1)
1.2 1 0.8 0.6 0.4 0.2 0
nrm ab

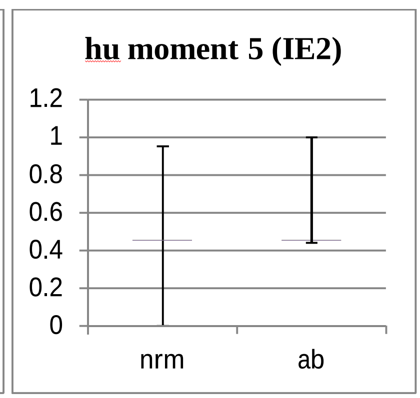
hu moment 5 (IE2)
1.2 1 0.8 0.6 0.4 0.2 0
nrm ab

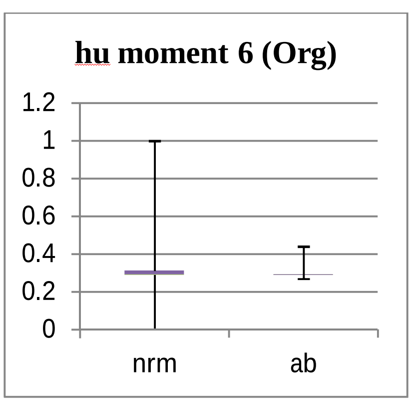
hu moment 6 (Org)
1.2 1 0.8 0.6 0.4 0.2 0
nrm ab

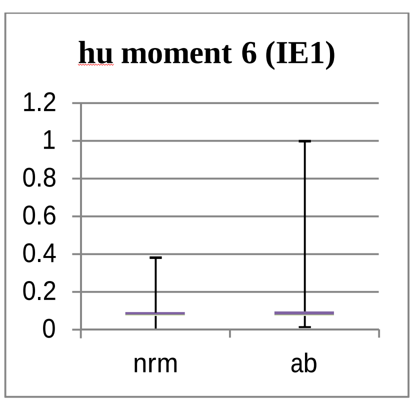
hu moment 6 (IE1)
1.2 1 0.8 0.6 0.4 0.2 0
nrm ab

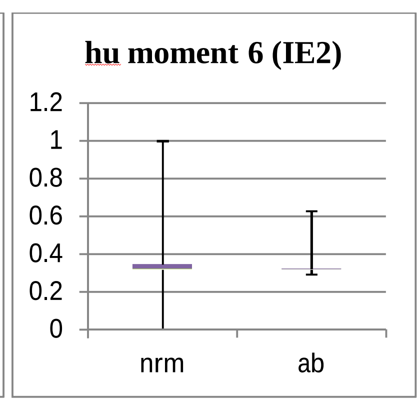
hu moment 6 (IE2)
1.2 1 0.8 0.6 0.4 0.2 0
nrm ab

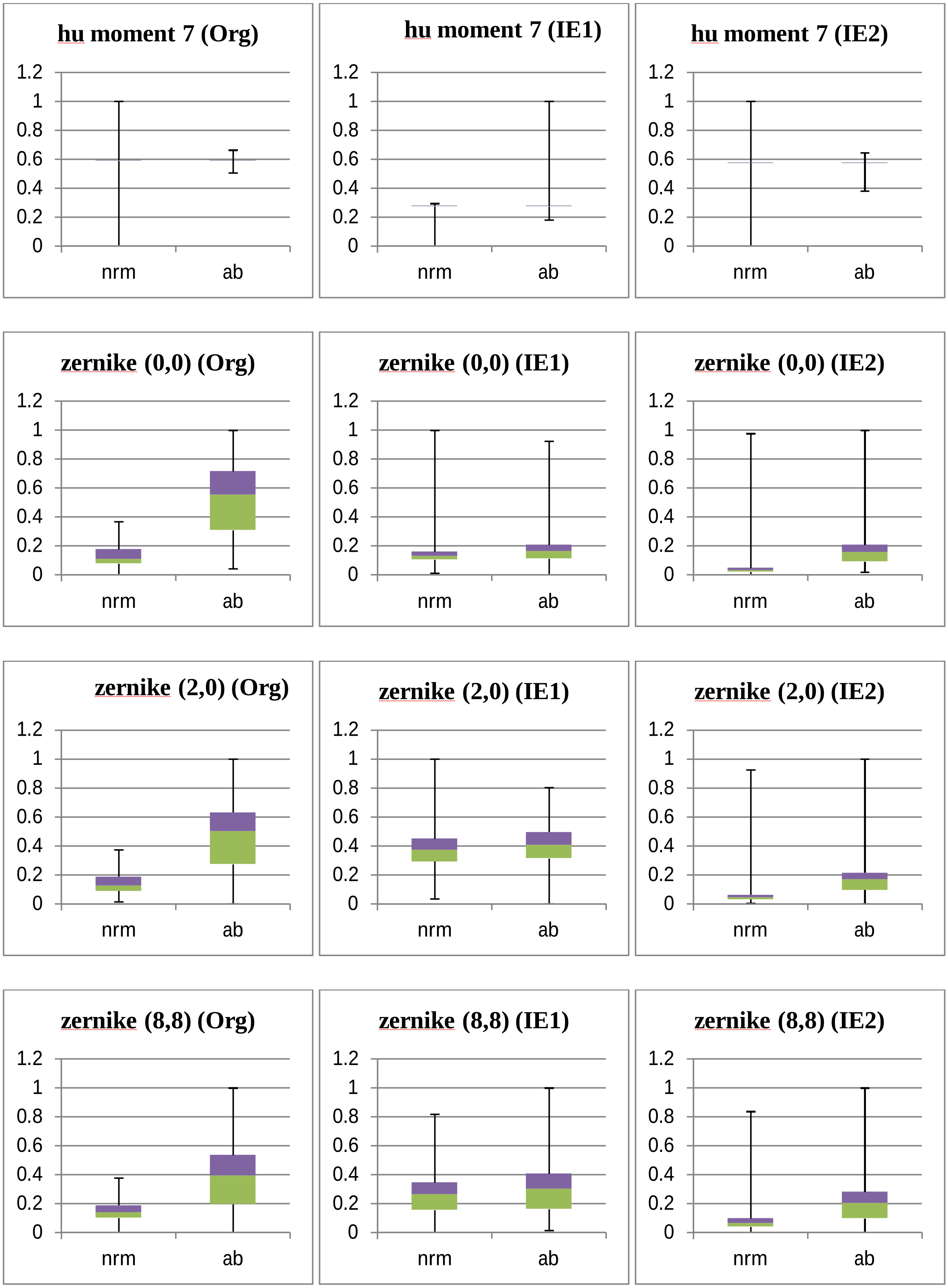
hu moment 7 (Org)
hu moment 7 (IE1)
hu moment 7 (IE2)
zernike (0,0) (Org)
zernike (0,0) (IE1)
zernike (0,0) (IE2)
zernike (2,0) (Org)
zernike (2,0) (IE1)
zernike (2,0) (IE2)
zernike (8,8) (Org)
zernike (8,8) (IE1)
zernike (8,8) (IE2)
1.2
1
0.8
0.6
0.4
0.2
0
nrm
ab

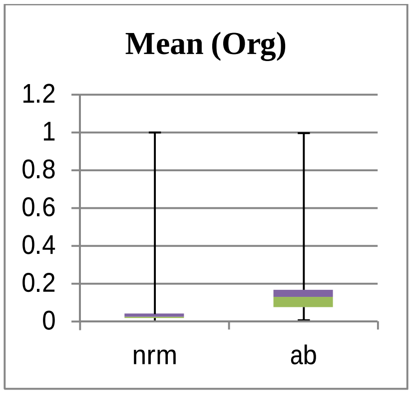
Mean (Org)
1.2
1
0.8
0.6
0.4
0.2
0
nrm
ab

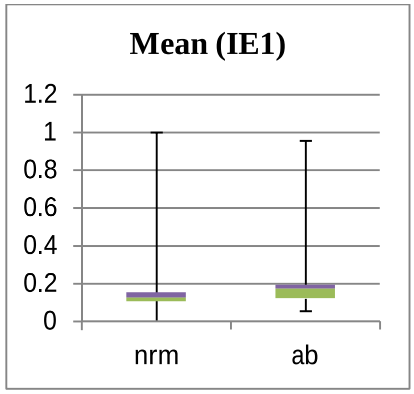
Mean (IE1)
1.2
1
0.8
0.6
0.4
0.2
0
nrm
ab

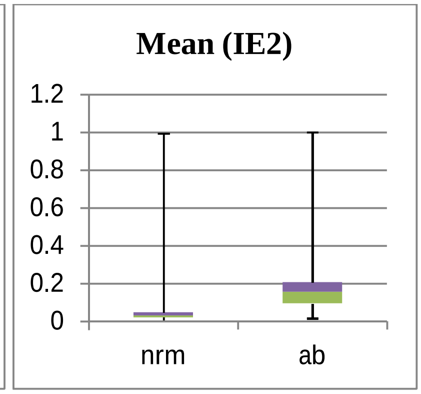
Mean (IE2)
1.2
1
0.8
0.6
0.4
0.2
0
nrm
ab

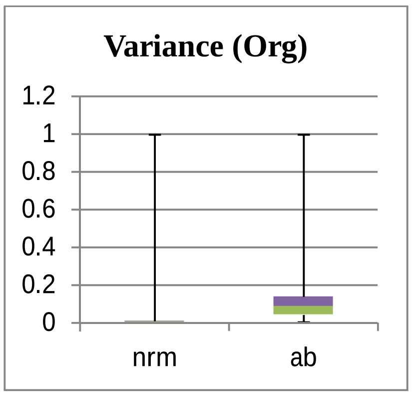
Variance (Org)
1.2
1
0.8
0.6
0.4
0.2
0
nrm
ab

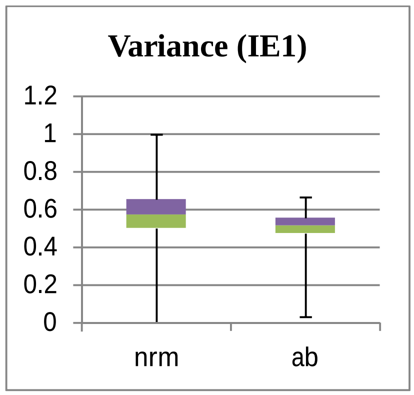
Variance (IE1)
1.2
1
0.8
0.6
0.4
0.2
0
nrm
ab

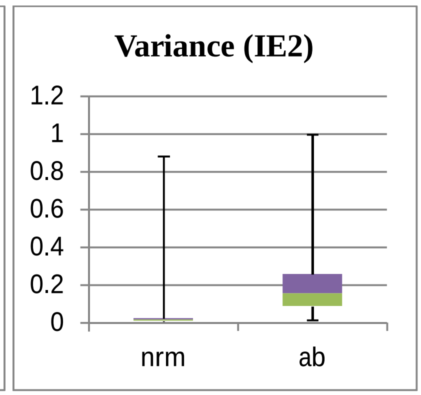
Variance (IE2)
1.2
1
0.8
0.6
0.4
0.2
0
nrm
ab

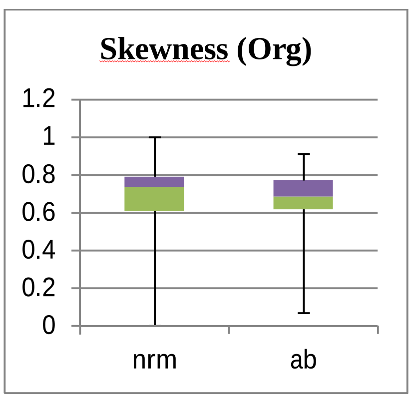
Skewness (Org)
1.2
1
0.8
0.6
0.4
0.2
0
nrm
ab

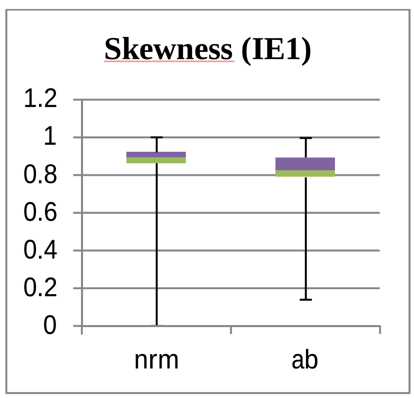
Skewness (IE1)
1.2
1
0.8
0.6
0.4
0.2
0
nrm
ab

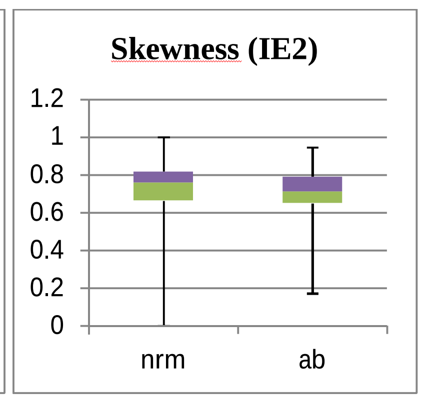
Skewness (IE2)
1.2
1
0.8
0.6
0.4
0.2
0
nrm
ab

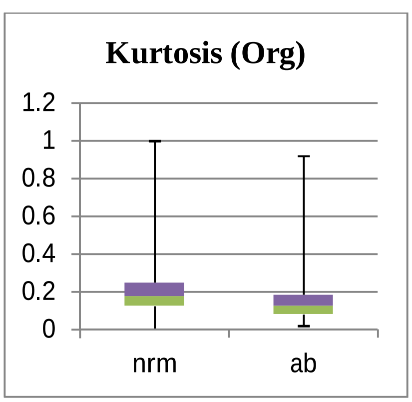
Kurtosis (Org)
1.2
1
0.8
0.6
0.4
0.2
0
nrm
ab

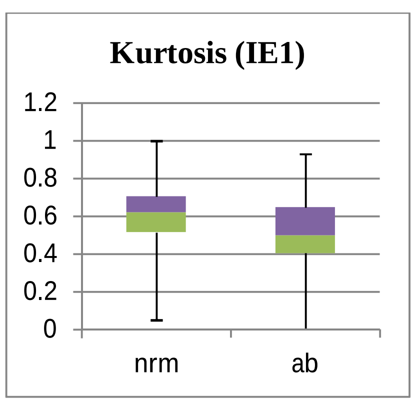
Kurtosis (IE1)
1.2
1
0.8
0.6
0.4
0.2
0
nrm
ab

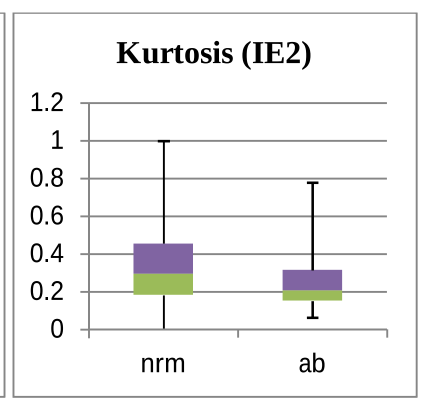
Kurtosis (IE2)
1.2
1
0.8
0.6
0.4
0.2
0
nrm
ab

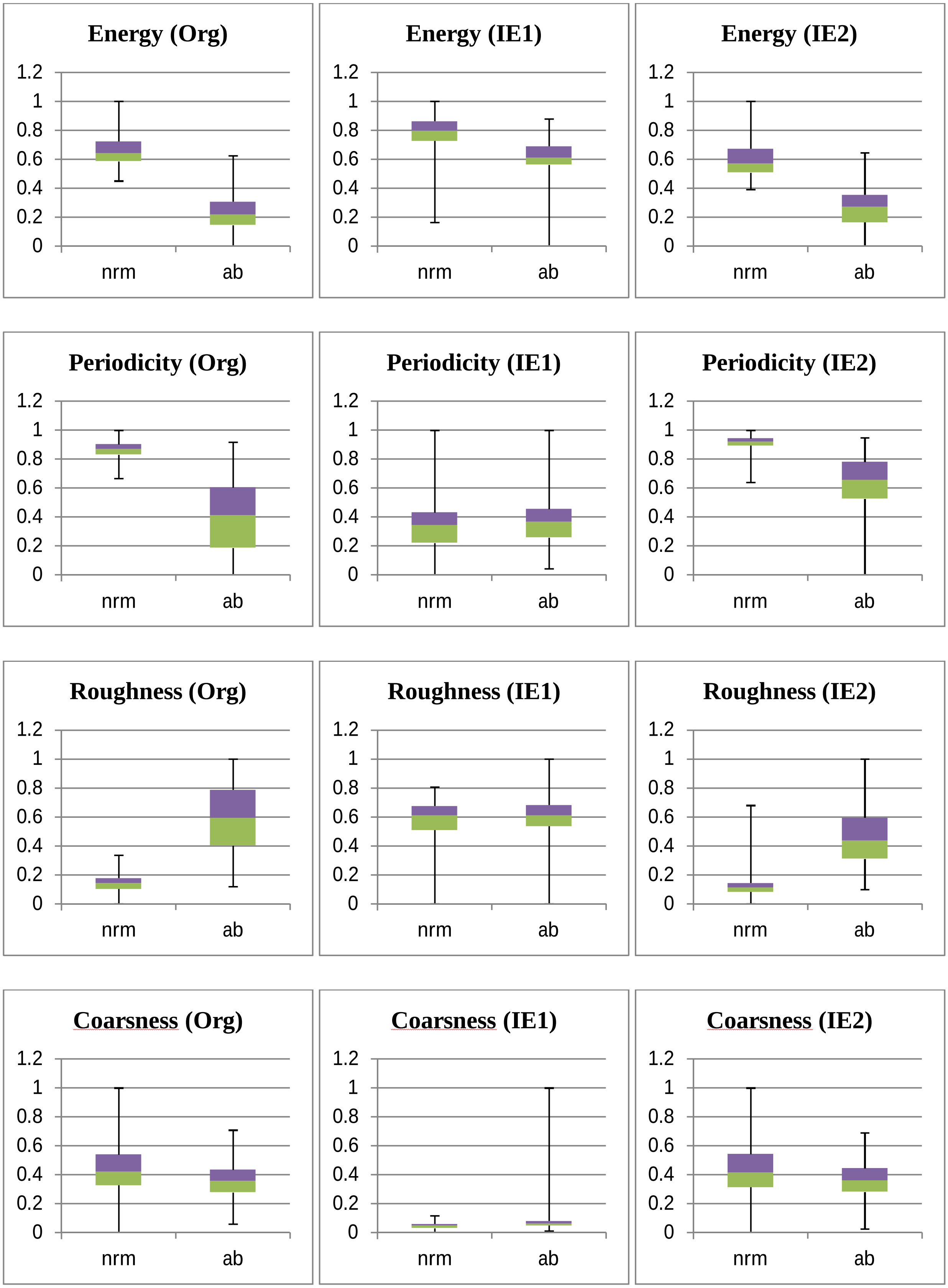
Energy (Org)
Energy (IE1)
Energy (IE2)
Periodicity (Org)
Periodicity (IE1)
Periodicity (IE2)
Roughness (Org)
Roughness (IE1)
Roughness (IE2)
Coarsness (Org)
Coarsness (IE1)
Coarsness (IE2)
0
0.2
0.4
0.6
0.8
1
1.2
nrm
ab

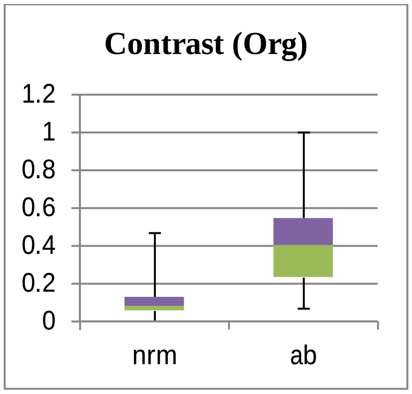
Contrast (Org)
1.2
1
0.8
0.6
0.4
0.2
0
nrm
ab

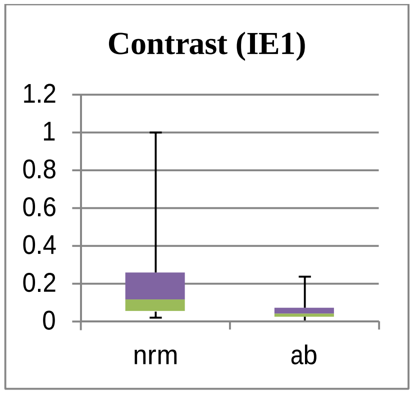
Contrast (IE1)
1.2
1
0.8
0.6
0.4
0.2
0
nrm
ab

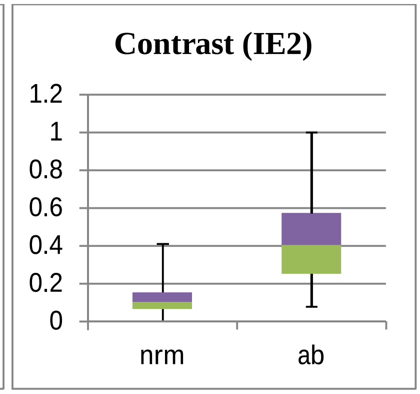
Contrast (IE2)
1.2
1
0.8
0.6
0.4
0.2
0
nrm
ab

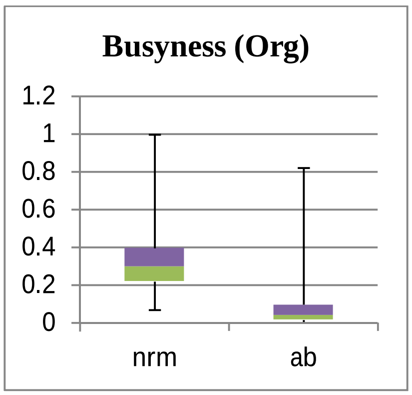
Busyness (Org)
1.2
1
0.8
0.6
0.4
0.2
0
nrm
ab

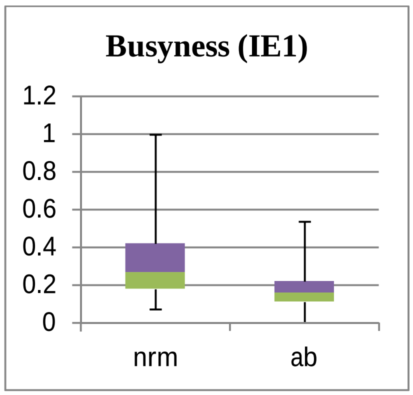
Busyness (IE1)
1.2
1
0.8
0.6
0.4
0.2
0
nrm
ab

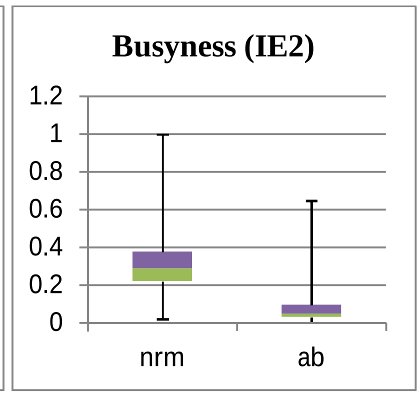
Busyness (IE2)
1.2
1
0.8
0.6
0.4
0.2
0
nrm
ab

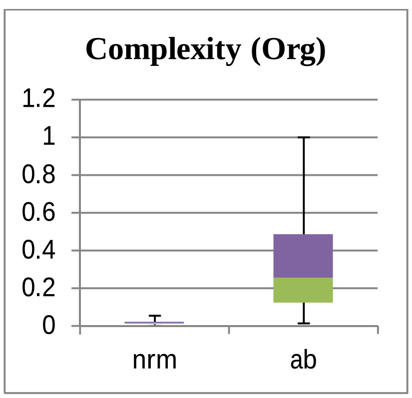
Complexity (Org)
1.2
1
0.8
0.6
0.4
0.2
0
nrm
ab

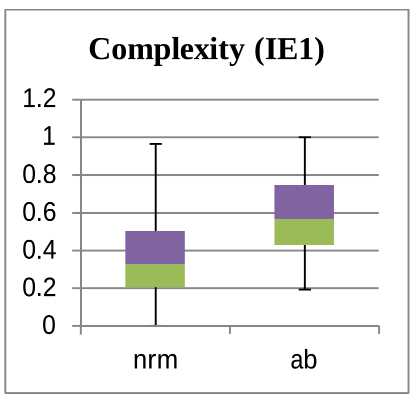
Complexity (IE1)
1.2
1
0.8
0.6
0.4
0.2
0
nrm
ab

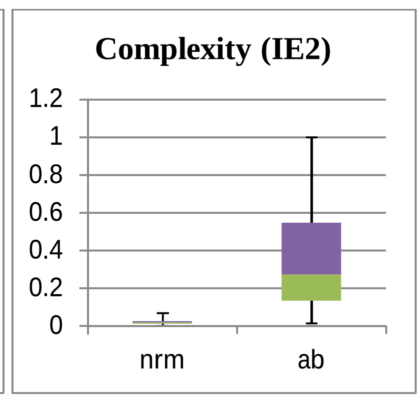
Complexity (IE2)
1.2
1
0.8
0.6
0.4
0.2
0
nrm
ab

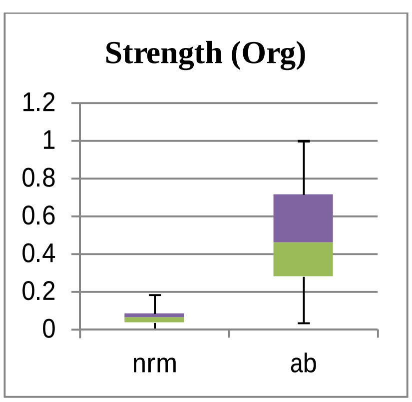
Strength (Org)
1.2
1
0.8
0.6
0.4
0.2
0
nrm
ab

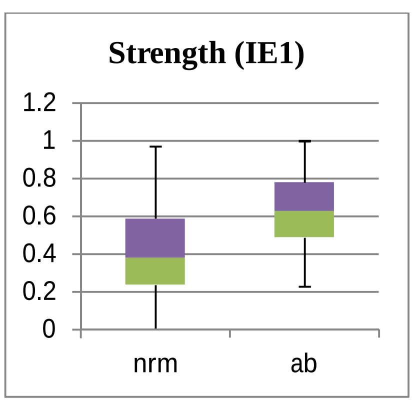
Strength (IE1)
1.2
1
0.8
0.6
0.4
0.2
0
nrm
ab

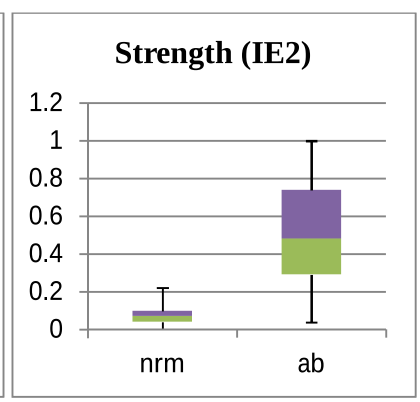
Strength (IE2)
1.2
1
0.8
0.6
0.4
0.2
0
nrm
ab

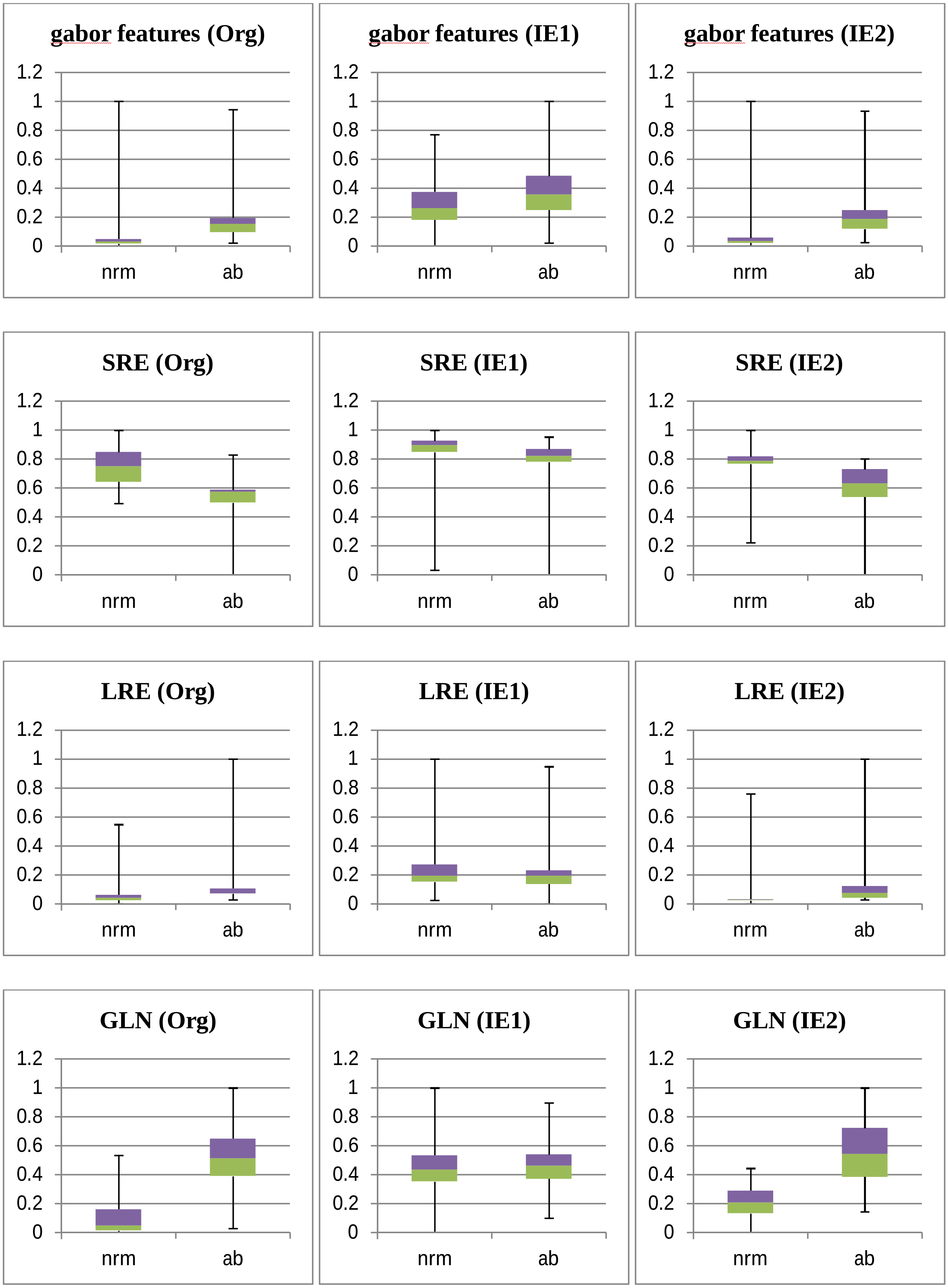
gabor features (Org)
gabor features (IE1)
gabor features (IE2)
SRE (Org)
SRE (IE1)
SRE (IE2)
LRE (Org)
LRE (IE1)
LRE (IE2)
GLN (Org)
GLN (IE1)
GLN (IE2)
1.2
1
0.8
0.6
0.4
0.2
0
nrm
ab

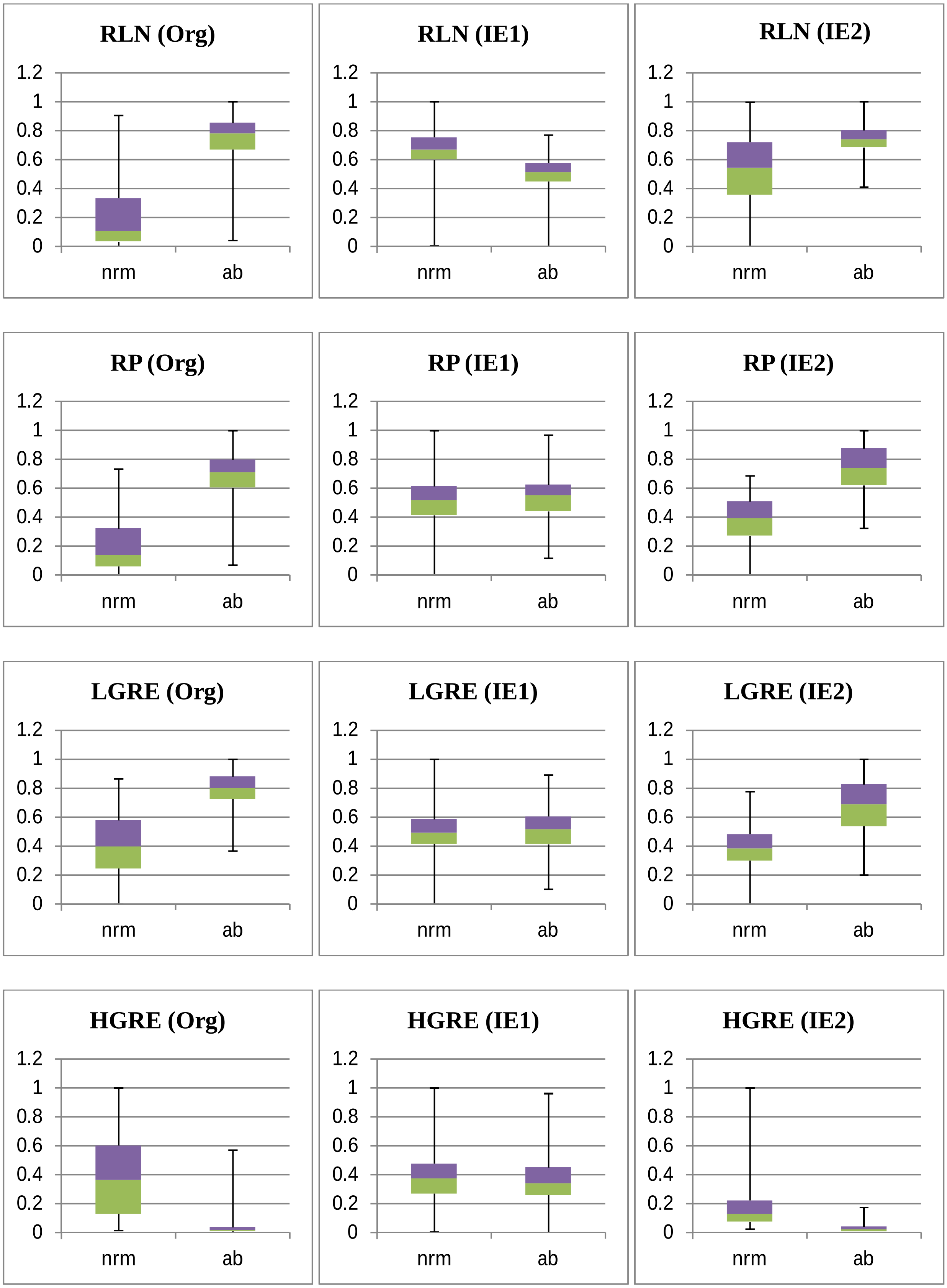
RLN (Org)
RLN (IE1)
RLN (IE2)
RP (Org)
RP (IE1)
RP (IE2)
LGRE (Org)
LGRE (IE1)
LGRE (IE2)
HGRE (Org)
HGRE (IE1)
HGRE (IE2)
1.2
1
0.8
0.6
0.4
0.2
0
nrm
ab

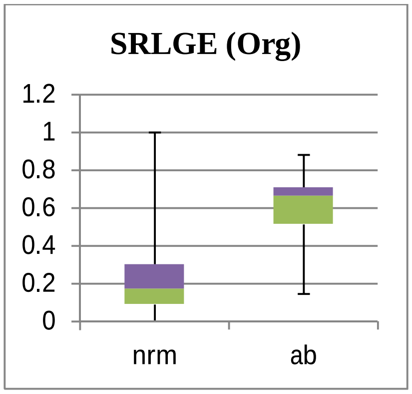
SRLGE (Org)
1.2
1
0.8
0.6
0.4
0.2
0
nrm
ab

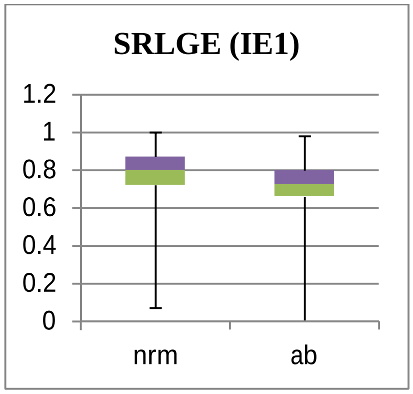
SRLGE (IE1)
1.2
1
0.8
0.6
0.4
0.2
0
nrm
ab

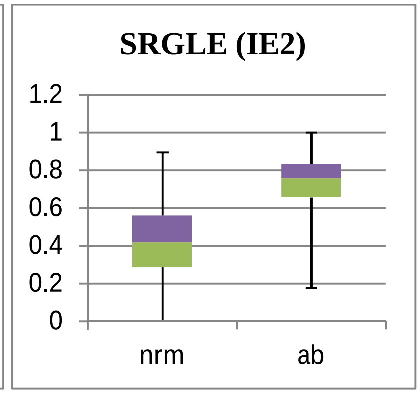
SRGLE (IE2)
1.2
1
0.8
0.6
0.4
0.2
0
nrm
ab

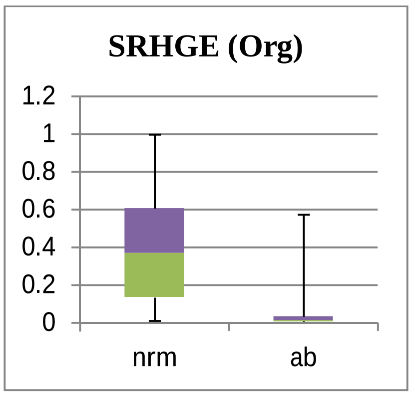
SRHGE (Org)
1.2
1
0.8
0.6
0.4
0.2
0
nrm
ab

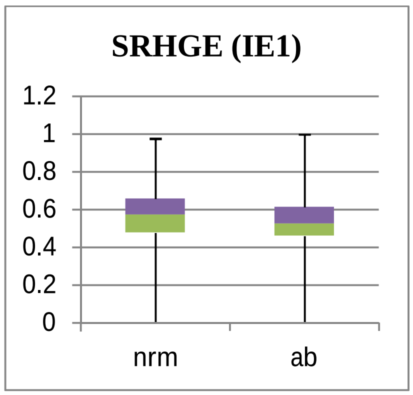
SRHGE (IE1)
1.2
1
0.8
0.6
0.4
0.2
0
nrm
ab

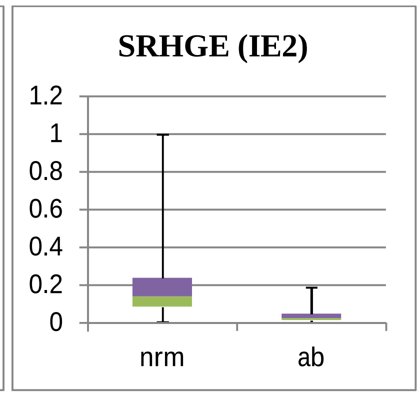
SRHGE (IE2)
1.2
1
0.8
0.6
0.4
0.2
0
nrm
ab

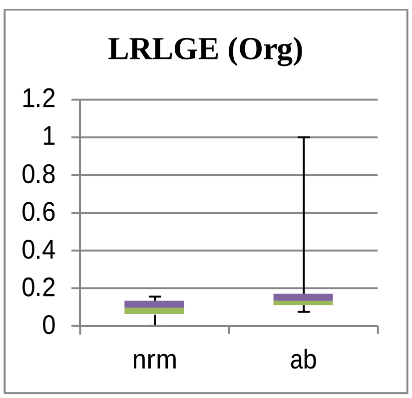
LRLGE (Org)
1.2
1
0.8
0.6
0.4
0.2
0
nrm
ab

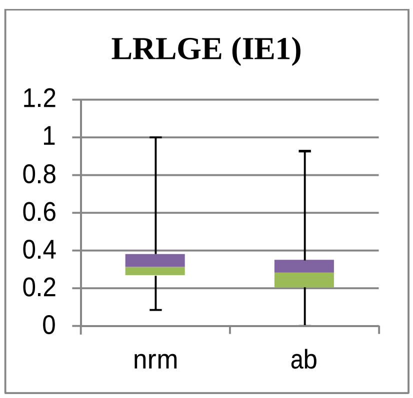
LRLGE (IE1)
1.2
1
0.8
0.6
0.4
0.2
0
nrm
ab

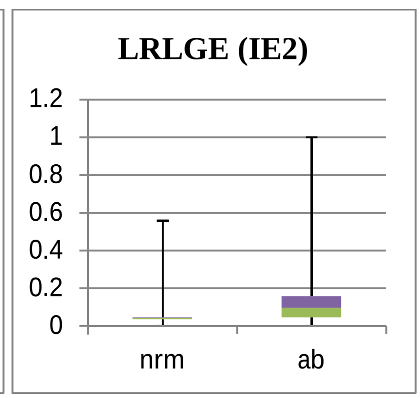
LRLGE (IE2)
1.2
1
0.8
0.6
0.4
0.2
0
nrm
ab

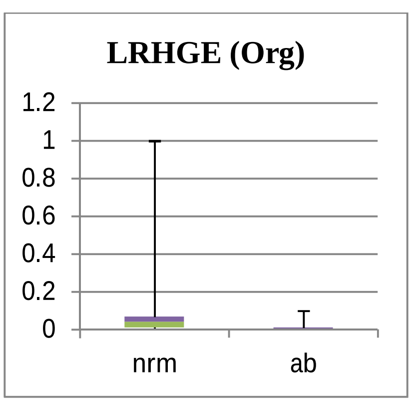
LRHGE (Org)
1.2
1
0.8
0.6
0.4
0.2
0
nrm
ab

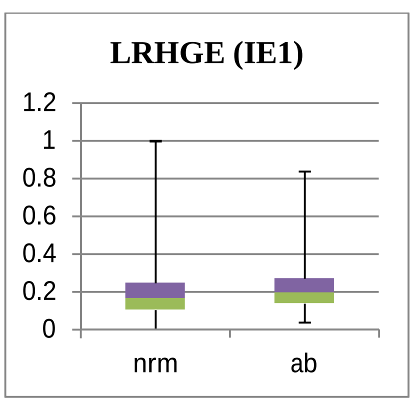
LRHGE (IE1)
1.2
1
0.8
0.6
0.4
0.2
0
nrm
ab

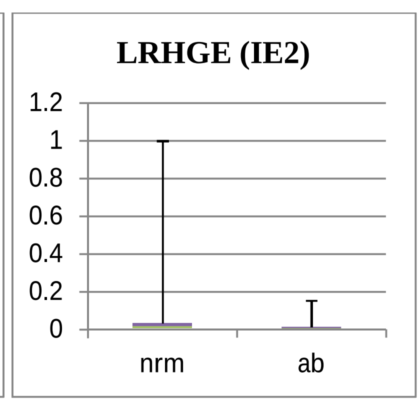
LRHGE (IE2)
1.2
1
0.8
0.6
0.4
0.2
0
nrm
ab